Published in Phys.Chem.Chem.Phys 2007, vol 9, p 2844-2855
DOI: 10.1039/b700913e

Computing steady-state metal flux at microorganism and bioanalogical sensor interfaces in multiligand systems. A reaction layer approximation and its comparison with the rigorous solution.

Jacques Buffle[a*], Konstantin Startchev[a], Josep Galceran[b]

[a] *Analytical and Biophysical Environmental Chemistry (CABE), Dept of Inorganic, Analytical and Applied Chemistry, Sciences II, 30 quai E. Ansermet, CH-1211 Geneva 4*

[b] *Departament de Quimica, University of Lleida, Rovira Roure 191, 25198 Lleida, Spain*

***** Corresponding author:

Jacques Buffle

Analytical and Biophysical Environmental Chemistry (CABE)

Department of Inorganic, Analytical and Applied Chemistry

Sciences II, 30 quai E. Ansermet, CH-1211 Geneva 4

Tel. ++41/22/379 6431 or ++44/22/379 6053

Fax ++ 41/22/ 379 6069

E-mail : Jacques.Buffle@cabe.unige.ch

Published in Phys.Chem.Chem.Phys 2007, vol 9, p 2844-2855
DOI: 10.1039/b700913e

Abstract

In complicated environmental or biological systems, the fluxes of chemical species at a consuming interface, like an organism or an analytical sensor, involve many coupled chemical and diffusion processes. Computation of such fluxes becomes, thus, difficult. The present paper describes an approximate approach, based on the so-called reaction layer concept, which enables to obtain a simple analytical solution for the steady-state flux of a metal ion at a consuming interface, in presence of many ligands, which are in excess with respect to the test metal ion. This model can be used for an unlimited number of ligands and complexes, without limit for the values of the association/dissociation rate constants or diffusion coefficients. This approximate solution is compared with a rigorous approach for the computation of the fluxes based on an extension of a previously published method. Comparison is performed for a very wide range of the key parameters: rate constants and diffusion coefficients, equilibrium constants and ligand concentrations. Their combined influence is studied in the whole domain of fully labile to non-labile complexes, via two combination parameters: the lability index, $\mathcal{L}$, and the reaction layer thickness, μ. The results show that the approximate solution provides accurate results in most cases. However, for particular combinations of metal complexes with specific values of $\mathcal{L}$ or μ, significant differences between the approximate and rigorous solutions may occur. They are evaluated and discussed. These results are important for three reasons: i) they enable to use the approximate solution in a fully reliable manner, ii) when present, the differences between approximate and rigorous solution are largely due to the coupling of chemical reactions, whose importance can thus be estimated, iii) due to its simple mathematical expression, the individual contribution of each metal species to the overall flux can be computed.

Published in Phys.Chem.Chem.Phys 2007, vol 9, p 2844-2855
DOI: 10.1039/b700913e

Key words

Flux of metal complexes, metal complex lability, multiligand system, reaction layer concept, reaction layer thickness, speciation, trace metal analysis, bioavailability

Introduction

In environmental and biological science, the computation of metal fluxes at consuming interfaces, such as microorganism surface [1-3], or bioanalogical sensors (also called dynamic sensors [4-8]) is of major importance to understand and predict the impact of metals on biota and ecosystems. Even though the role of the physicochemical properties of a single metal complex has been extensively studied [9-19], computation of metal flux in a real system containing a large number of different types of ligands is still very difficult[5;20-23]. Such computations however are of major importance to compare experimental data with theoretical predictions, in order to quantitatively understand the environmental and biological system functioning.

No user-friendly code for such flux computation (equivalent to the many codes existing for computing the distribution of metal complexes at equilibrium such as MINTEQ [24], MINEQL or MEDUSA [25]), have been yet developed. Metal flux computation in multi-ligand systems should consider three major types of physico-chemical processes: i) the dynamic process at the consuming interface, ii) the dynamics of diffusive mass-transport of the metal and ligand species in solution, and iii) their coupling via the chemical formation and dissociation kinetics of all complexes in the medium. Without speaking of the difficulty of getting realistic values for the corresponding parameters, in particular rate constants and diffusion coefficients [1], which is discussed in details elsewhere [26], mathematically solving a large number of diffusion/reaction equations, with parameter values varying by several orders of magnitudes,

is not straightforward [21;27]. Turner and Whitfield [20], and more recently Galceran et al. [22] developed a methodology to find, under different geometries, the exact steady-state solution under the condition of excess ligand concentration (compared to total metal concentration). This method (hereafter called rigorous solution = RS), however, requires relatively advanced mathematical operations (including numerical diagonalisation of large matrices), it is not easy to use by non-specialists and the physical meaning of the resulting expressions is not straightforward.

In the present work, we have developed an alternative simple method based on the reaction layer approximation (hereafter denoted as RLA). It is valid under excess of ligand and steady-state conditions i.e. when all concentration gradients inside the reactive-diffusion layer are independent of time. Its advantage over the RS is that i) the RLA leads to a simple (and intuitive) analytical mathematical solution for the overall flux, even for an unlimited number of ligands, so it is very easy to use by non specialists. ii) the individual contribution of each complex in the overall metal flux can be readily assessed from simple mathematical equations, iii) it works well in the case of large number of ligands, where alternative numerical procedures may have problems, especially when the kinetic parameters differ by many orders of magnitude, iv) computation time is negligible and v) it is readily implemented in computer codes or even in a spreadsheet such as Excel. Thus it might be a useful tool to study dynamic biophysico-chemical processes in ecosystems.

In order to evaluate the validity of the RLA for multiligand systems, we have developed a user-friendly software, called FLUXY, which can use either RLA or RS and which can compare both results. In this paper we present the fundamental basis of RLA as well as the results of a systematic comparison of RLA and RS results, computed over a very broad

domain of dynamic parameters of the metal complexes. These results are useful for two reasons:

a.- The major physico-chemical difference between the RLA and the RS approaches is that the RLA considers the formation/dissociation of the various metal complexes essentially as independent reactions, whereas in reality at any time and distance from the interface they are coupled through the concentration of the free metal ion. The difference between the RLA and RS results, thus, becomes an estimation of the importance of this coupling under the condition used. In multiligand systems, this estimation cannot readily be performed by simple observation of the characteristics of the complexes involved, because of the very large number of kinetic and thermodynamical parameters involved in an intricate manner in the overall flux. The present results show under which conditions this coupling is important, thus facilitating further systematic study and understanding of the corresponding physicochemical processes

b.- These results will show under which conditions the RLA can be used reliably, i.e. with minimal error, in complicated environmental systems. In fact they show that in most cases, the RLA provides a good approximation of the metal flux, sufficient for most environmental applications, in particular when considering the rather large uncertainties existing on the values of kinetic parameters.

2- Theory: application of the RLA to a multiligand system

The concept of reaction layer has been developed and systematically studied long time ago, in the field of polarography [28], and applied later to the computation of metal fluxes at organism surfaces [29]. It has been revisited in the recent years [17-19;30], but -except for a few

contributions [23;31;32] - it was applied to solutions containing a single ligand, L. This paper applies the concept of reaction layer to an unlimited mixture of ligands in excess compared to the metal and tests the validity of this approximation, under this condition.

For a system of one ligand L and one complex ML, in which only free M (and not ML) is consumed at the surface of a sphere of radius r_0, the basic assumption is the following (Fig.1): in the bulk solution and inside the reactive-diffusion layer (with thickness = δ), sufficiently far from the consuming surface, M and ML are in equilibrium with each other, and diffuse towards the surface, by keeping constant their relative proportion. This is the case all along the diffusion layer, from the consuming surface ($r = r_0$) up to $r = r_0+\delta$, when the complexes are fully labile, i.e. when association of M and L and dissociation of ML are very fast compared to the diffusion process. However, in a general case, within a solution layer of thickness μ in contact with the surface, the association/dissociation reactions of M and L are not fast enough to maintain the equilibrium when M is consumed at the interface. In the RLA, it is assumed that, inside this layer, M does not re-associate at all with L and only disappears by consumption at the surface. Thus in this layer, called reaction layer, the concentration of ML is also assumed to be constant, and the overall flux of M species is entirely supported by diffusion of M.

Figure 1 depicts the steady-state concentration profiles outside a spherical consuming surface, for a multiligand and multicomplex system, exemplified by 2 ligands, ^{1}L, and ^{2}L, forming only 1/1 complexes, M^{1}L and M^{2}L. The chemical rates are in the order: M^{1}L > M^{2}L and thus the reaction layer thicknesses are in the order $\mu_1 < \mu_2$ (eq.(1)). By definition, any complex such that $\mu > \delta$ is taken as a so-called non-labile (or inert) complex: its concentration remains constant in the whole diffusion layer and is equal to that in the bulk solution. Thus, its

Published in Phys.Chem.Chem.Phys 2007, vol 9, p 2844-2855
DOI: 10.1039/b700913e

contribution to the flux is taken as nil. At $r < r_0 + \mu_1$, the diffusive flux is only supported by free M, while for $r_0 + \mu_1 < r < r_0 + \mu_2$, the diffusive flux is supported by the diffusion of M and M^1L, and for $r_0 + \mu_2 < r < r_0 + \delta$, the flux is supported by $M + M^1L + M^2L$. Of course, at each side of the boundaries $r = r_0 + \mu_1$ and $r = r_0 + \mu_2$, the total metal fluxes should be equal. As mentioned in the introduction, this approach neglects the coupling of the formation/dissociation of M^1L and M^2L due to the interconversion of M^1L and M^2L via free M.

2.1. Flux of labile and semilabile complexes ($\mu \leq \delta$) at a spherical consuming surface

For a 1/1 complex, M^iL, in a solution containing an excess of ligand, ^iL, compared to M, it has been shown, first for planar diffusion [11-13;28] and later for spherical semi-infinite diffusion [17], that the reaction layer thickness, μ_i, is given by:

$$\mu_i = \sqrt{\frac{D_M}{{}^i k_a \, [{}^iL]}} \tag{1}$$

where D_M is the diffusion coefficient of free M, $[{}^iL]$ the concentration of free ^iL, and ^ik_a is the association rate constant of M and ^iL to form M^iL. For most simple inorganic or organic ligands, successive complexes M^iL_k may be formed, where k is a stoichiometric integer ($k \geq 1$). In most cases for simple ligands, the chemical kinetics of complexes M^iL_k with $k > 1$ is faster than those of M^iL. For example, in the reaction layer, $[M^iL_2]$ and $[M^iL]$ are related by (see eqn. (28) in [31]):

$$[M^iL_2] = [M^iL] \left({}^iK_2[{}^iL] + \frac{{}^ik_{d,1}}{{}^ik_{d,2}} \right) \tag{2}$$

where $^iK_2$ is the formation stability constant of M^iL_2 from M^iL and $^ik_{d,1}$ and $^ik_{d,2}$ are the dissociation rate constants of M^iL and M^iL_2 respectively. In most cases $^ik_{d,1} < {}^ik_{d,2}$ and in addition, M^iL_2 is important only when $^iK_2[{}^iL] > 1$. Thus, in practical cases, the second term

in the parenthesis of eq. (2) can be neglected and an equilibrium relationship exists between M^iL and M^iL_2. The same reasoning is applicable to complexes with higher k values. Thus it can be assumed with a good approximation that i) all complexes M^iL_k are in equilibrium with each other, inside and outside the reaction layer, and ii) the thickness of the reaction layer for all the complexes with ligand ^iL is given by equation (1), i.e. it is controlled by the association kinetics of the 1/1 complex M^iL.

The flux at the consuming surface is computed below assuming:

a.- a solution containing M and the two ligands ^1L and ^2L (Figure 1), and

b.- a spherical interface where the rate of consumption of M on the sphere is supposed to be proportional to the free M concentration at the surface, $[M]_0$. A relevant example is the case of metal uptake by a spherical microorganism, when the transport sites at the membrane surface, R, are far from being saturated by M[1]. Then the internalisation flux, J_{int} is given by:

$$J_{int} = k_{int}\{MR\} = k_{int}K_a\{R\}[M]_0 \quad (3)$$

where K_a is the surface complexation constant of M with the transport site R, and {R} is their surface concentration.

The equation will be generalized to an unlimited number of ligands (see below) and to planar surfaces (section 2.2).

Because of the mass conservation condition, the total number of moles of species M transported per time unit, F, through any spherical surface area, with the same centre as the consuming sphere, is constant. In particular, at the surface located at $r = r_0$, $r = r_0+\mu_1$ and $r = r_0 + \mu_2$, one gets:

Published in Phys.Chem.Chem.Phys 2007, vol 9, p 2844-2855
DOI: 10.1039/b700913e

$$F = 4\pi r_0^2 J_{\text{int}} = 4\pi r_0^2 J_{r_0} = 4\pi \left(r_0 + \mu_1\right)^2 J_{r_0+\mu_1} = 4\pi \left(r_0 + \mu_2\right)^2 J_{r_0+\mu_2} \quad (4)$$

where J_{int}, J_{r_0}, $J_{r_0+\mu_1}$ and $J_{r_0+\mu_2}$ are the internalisation flux and the diffusive fluxes crossing a spherical surface at $r=r_0$ (J_{r_0}), at $r=r_0+\mu_1$ ($J_{r_0+\mu_1}$) and at $r=r_0+\mu_2$ ($J_{r_0+\mu_2}$). The various diffusive fluxes can be computed as explained below (definitions are compiled in a short Table of symbols and with more detail in Appendix A).

For $r_0 \le r \le r_0 + \mu_1$ at steady state, Fick's second law prescribes

$$D_{\text{M}} \left(\frac{\partial^2 [\text{M}]}{\partial r^2} + \frac{2}{r} \frac{\partial [\text{M}]}{\partial r} \right) = \nabla^2 (D_{\text{M}} [\text{M}]) = \nabla^2 \chi = 0 \quad (5)$$

where ∇^2 is the Laplacian operator for spherical geometry and [M] is the concentration of free M. The solution of this equation, with $\chi = D_{\text{M}} [\text{M}]$, is

$$\chi = G + \frac{B}{r} \quad (6)$$

where G and B are constants. The boundary conditions are $[\text{M}] = [\text{M}]_0$ at $r = r_0$ leading to $\chi_0 = G + B / r_0$, and $[\text{M}] = [\text{M}]_{\mu_1}$ at $r = r_0 + \mu_1$ leading to $\chi_{\mu_1} = G + B/(r_0 + \mu_1)$. Thus one obtains:

$$\chi_{\mu_1} - \chi_0 = B \left(\frac{1}{r_0 + \mu_1} - \frac{1}{r_0} \right) \quad (7)$$

and, by differentiation of eq. (6):

$$\frac{\partial \chi}{\partial r} = -\frac{B}{r^2} \quad (8)$$

Combining eqs (7) and(8) at $r = r_0$ gives :

$$J_{r_0} = \left(\frac{\partial \chi}{\partial r}\right)_{r=r_0} = \frac{D_{\mathrm{M}}\left([\mathrm{M}]_{\mu_1} - [\mathrm{M}]_0\right)}{r_0^2\left(\frac{1}{r_0} - \frac{1}{r_0+\mu_1}\right)} \tag{9}$$

and

$$F = 4\pi r_0^2 J_{r_0} = \frac{4\pi D_{\mathrm{M}}\left([\mathrm{M}]_{\mu_1} - [\mathrm{M}]_0\right)}{\frac{1}{r_0} - \frac{1}{r_0+\mu_1}} \tag{10}$$

Between r_0 + μ_1 and r_0 + μ_2, the diffusive species are M and all n_1 successive complexes M^1L_k (note that only M^1L is shown in Fig. 1). Fick's law becomes:

$$\nabla^2 \chi = \nabla^2\left(D_{\mathrm{M}}[\mathrm{M}] + \sum_{k=1}^{n_1} D_{\mathrm{M}^1\mathrm{L}_k}[\mathrm{M}^1\mathrm{L}_k]\right) = 0 \tag{11}$$

The solution is given by eq (6), where the constants *G* and *B* are now computed from the boundary conditions at $r = r_0 + \mu_1$ ($[\mathrm{M}] = [\mathrm{M}]_{\mu_1}$; $[\mathrm{M}^1\mathrm{L}_k] = [\mathrm{M}^1\mathrm{L}_k]_{\mu_1}$) and at $r = r_0 + \mu_2$ ($[\mathrm{M}] = [\mathrm{M}]_{\mu_2}$; $[\mathrm{M}^1\mathrm{L}_k] = [\mathrm{M}^1\mathrm{L}_k]_{\mu_2}$). The diffusive flux through the surface at $r = r_0 + \mu_1$ is

$$J_{r_0+\mu_1} = \left(\frac{\partial \chi}{\partial r}\right)_{r_0+\mu_1} \tag{12}$$

and using the same algebraic manipulation as before, one gets:

$$F = 4\pi\left(r_0 + \mu_1\right)^2 J_{r_0+\mu_1} = \frac{4\pi\left(D_{\mathrm{M}} + \dot{D}_1\gamma_1\right)\left([\mathrm{M}]_{\mu_2} - [\mathrm{M}]_{\mu_1}\right)}{\left(\frac{1}{r_0+\mu_1} - \frac{1}{r_0+\mu_2}\right)} \tag{13}$$

where γ_1 is :

$$\gamma_1 = \sum_{k=1}^{n_1} {}^1\beta_k [{}^1\mathrm{L}]^k \tag{14}$$

and the cumulative stability constants $^1\beta_k$ is:

$$ {}^1\beta_k = \frac{[\mathrm{M}^1\mathrm{L}_k]}{[\mathrm{M}][{}^1\mathrm{L}]^k} \tag{15} $$

$\dot{D}_1$ is an average diffusion coefficient for the whole of the complexes $\mathrm{M}^1\mathrm{L}_k$, weighted by the proportion of each complex $\mathrm{M}^1\mathrm{L}_k$ i.e. :

$$ \dot{D}_1 = D_{\mathrm{M}^1\mathrm{L}} \frac{[\mathrm{M}^1\mathrm{L}]}{\sum_{k=1}^{n_1}[\mathrm{M}^1\mathrm{L}_k]} + D_{\mathrm{M}^1\mathrm{L}_2} \frac{[\mathrm{M}^1\mathrm{L}_2]}{\sum_{k=1}^{n_1}[\mathrm{M}^1\mathrm{L}_k]} + .. + D_{\mathrm{M}^1\mathrm{L}_n} \frac{[\mathrm{M}^1\mathrm{L}_{n_1}]}{\sum_{k=1}^{n_1}[\mathrm{M}^1\mathrm{L}_k]} \tag{16} $$

The same procedure can be used to compute the diffusive flux for $r_0 + \mu_2 \le r \le r_0 + \delta$. The diffusive species (Fig. 1) are M and all the complexes $\mathrm{M}^1\mathrm{L}_k$ and $\mathrm{M}^2\mathrm{L}_{k'}$. Fick's law becomes:

$$ \nabla^2 \chi = \nabla^2 \left(D_{\mathrm{M}}[\mathrm{M}] + \sum_{k=1}^{n_1} D_{\mathrm{M}^1\mathrm{L}_k}[\mathrm{M}^1\mathrm{L}_k] + \sum_{k'=1}^{n_2} D_{\mathrm{M}^2\mathrm{L}_{k'}}[\mathrm{M}^2\mathrm{L}_{k'}] \right) = 0 \tag{17} $$

By using the same procedure as before, one gets F at the surface $r_0 + \mu_2$:

$$ F = 4\pi\left(r_0 + \mu_2\right)^2 J_{r_0+\mu_2} = \frac{4\pi\left(D_{\mathrm{M}} + \dot{D}_1\gamma_1 + \dot{D}_2\gamma_2 \right)\left([\mathrm{M}]^* - [\mathrm{M}]_{\mu_2}\right)}{\left(\frac{1}{r_0+\mu} - \frac{1}{r_0+\delta}\right)} \tag{18} $$

where $[\mathrm{M}]^*$ is the concentration of free M in the bulk solution, and $\dot{D}_1\gamma_1$ and $\dot{D}_2\gamma_2$ are given by eqs (14) to (16) with subscripts 1 and 2 respectively.

The flux at the interface, $J_{r_0} = F/\left(4\pi r_0^2\right)$, can be expressed as a function of $[\mathrm{M}]^*$, by combining eqs (3), (4), (10), (13) and (18) to eliminate $[\mathrm{M}]_0$, $[\mathrm{M}]_{\mu_1}$ and $[\mathrm{M}]_{\mu_2}$:

$$ J_{r_0} = \frac{[\mathrm{M}]^*}{\frac{r_0^2}{\overline{D_2}\alpha_2}\left(\frac{1}{r_0+\mu_2} - \frac{1}{r_0+\delta}\right) + \frac{r_0^2}{\overline{D_1}\alpha_1}\left(\frac{1}{r_0+\mu_1} - \frac{1}{r_0+\mu_2}\right) + \frac{r_0^2}{D_{\mathrm{M}}}\left(\frac{1}{r_0} - \frac{1}{r_0+\mu_1}\right) + \frac{1}{k_{\mathrm{int}}K_{\mathrm{a}}\{\mathrm{R}\}}} \tag{19} $$

where

Published in Phys.Chem.Chem.Phys 2007, vol 9, p 2844-2855
DOI: 10.1039/b700913e

$$\overline{D_i}\,\alpha_i = \sum_{j=0}^{i} \overset{\bullet}{D}_j \gamma_j \tag{20}$$

with $\overset{\bullet}{D}_0 = \mathrm{D_M}$, $\gamma_0 = 1$,

$$\overline{D_i} = \left(D_{\mathrm{M}}[\mathrm{M}] + \sum_{j=1}^{i}\sum_{k=1}^{n_j} D_{\mathrm{M}^{\,i}\mathrm{L}_k}[\mathrm{M}^{\,i}\mathrm{L}_k] \right) \Bigg/ \left([\mathrm{M}] + \sum_{j=1}^{i}\sum_{k=1}^{n_j} [\mathrm{M}^{\,i}\mathrm{L}_k] \right) \tag{21}$$

$$\alpha_i = 1 + \sum_{j=1}^{i} \gamma_i = 1 + \sum_{j=1}^{i}\sum_{k=1}^{n_j} {}^{j}\beta_k [{}^{j}\mathrm{L}]^k = \frac{1}{[\mathrm{M}]} \quad \left([\mathrm{M}] + \sum_{j=1}^{i}\sum_{k=1}^{n_j} [\mathrm{M}^{\,i}\mathrm{L}_k] \right) \tag{22}$$

and

$${}^{j}\beta_{k} = \frac{[\mathrm{M}^{\,j}\mathrm{L}_k]}{[\mathrm{M}][{}^{j}\mathrm{L}]^k} \tag{23}$$

For a system with two ligands, ^{1}L and ^{2}L, with n_1 and n_2 successive complexes respectively, the total concentration of M in the bulk solution, $[\mathrm{M}]_\mathrm{t}^*$, is related to [M]* by:

$$[\mathrm{M}]_\mathrm{t}^* = [\mathrm{M}]^* \left(1 + \sum_{k=1}^{n_1} {}^{1}\beta_k [{}^{1}\mathrm{L}]^k + \sum_{k=1}^{n_2} {}^{2}\beta_k [{}^{2}\mathrm{L}]^k \right) = [\mathrm{M}]^* \alpha_m \tag{24}$$

where m is the total number of different ligands in the medium (i.e. m = 2 in eqs (19), (24)). By rearranging the denominator of eq. (19) and combining eqs (19) and (24), one gets:

$$J_{r_0} = \frac{[\mathrm{M}]_\mathrm{t}^*}{\dfrac{\alpha_m}{k_{\mathrm{int}} K_\mathrm{a} \{\mathrm{R}\}} + \dfrac{r_0 \alpha_m}{D_\mathrm{M}} - \dfrac{r_0^2}{r_0 + \delta}\left(\dfrac{\alpha_m}{\overline{D_2}\alpha_2} \right) + \dfrac{r_0^2}{r_0 + \mu_1}\left(\dfrac{\alpha_m}{\overline{D_1}\alpha_1} - \dfrac{\alpha_m}{D_\mathrm{M}} \right) + \dfrac{r_0^2}{r_0 + \mu_2}\left(\dfrac{\alpha_m}{\overline{D_2}\alpha_2} - \dfrac{\alpha_m}{\overline{D_1}\alpha_1} \right)} \tag{25}$$

This equation can be generalized for a mixture of m ligands ^{i}L, which should be sorted out in the order of increasing μ_i values (slower and slower complexes), by using the general equations for ${}^{j}\beta$ and $\overline{D_i}\,\alpha_i$ (see eq. (20)) and for α_m:

Published in Phys.Chem.Chem.Phys 2007, vol 9, p 2844-2855
DOI: 10.1039/b700913e

$$\left[\mathrm{M}\right]_{\mathrm{t}}^{*} = \left[\mathrm{M}\right]^{*} + \sum_{j=1}^{m}\sum_{k=1}^{n_j}\left[\mathrm{M}^{j}\mathrm{L}_{k}\right]^{*} = \left[\mathrm{M}\right]^{*}\left(1 + \sum_{j=1}^{m}\sum_{k=1}^{n_j} {}^{j}\beta_{k}\left[{}^{j}\mathrm{L}\right]^{k}\right) = \left[\mathrm{M}\right]^{*}\alpha_{m} \tag{26}$$

In the denominator of eq. (25), derived for the particular case m=2, $\overline{D}_2\alpha_2$ corresponds to the ligand whose reaction layer thickness is larger than any other μ_i. In the general case, this corresponds to the ligand ${}^{m}\mathrm{L}$. Thus in eq. (25), $\overline{D}_2\alpha_2 = \overline{D}_m\alpha_m$. Consequently, the 4th and 5th terms of eq (25) can also be written as:

$$\alpha_m \sum_{i=1}^{m} \frac{r_0^2}{r_0 + \mu_i}\left(\frac{1}{\overline{D}_i\alpha_i} - \frac{1}{\overline{D}_{i-1}\alpha_{i-1}}\right) \tag{27}$$

with the ligands ${}^{i}\mathrm{L}$, sorted out in the order of increasing μ_i, i.e. of decreasing association rate constant (eq.(1)). Thus, by rearranging the numerator, eq. (25) becomes:

$$\boxed{J = \frac{\left[\mathrm{M}\right]_{\mathrm{t}}^{*}/\alpha_m}{\tau}} \tag{28}$$

with

$$\tau = \underbrace{\frac{1}{k_{\mathrm{int}}K_{\mathrm{a}}\{R\}}}_{\tau_1} + \underbrace{\frac{r_0}{\overline{D}_m\alpha_m}\left(\frac{\delta}{r_0+\delta}\right)}_{\tau_2} + \underbrace{\frac{r_0}{D_{\mathrm{M}}} - \frac{r_0}{\overline{D}_m\alpha_m} + \sum_{i=1}^{m}\frac{r_0^2}{r_0+\mu_i}\left(\frac{1}{\overline{D}_i\alpha_i} - \frac{1}{\overline{D}_{i-1}\alpha_{i-1}}\right)}_{\tau_3} \tag{29}$$

where $\overline{D}_0 = D_{\mathrm{M}}$ and $\alpha_0 = 1$. τ has units of [time/length] and is the reciprocal of an overall rate of mass transport of M species. It is composed of three terms, τ_1, τ_2 and τ_3, corresponding to three types of rate limiting processes:

1- a rate limiting interfacial transport (Fig. 1) is characterized by $k_{\mathrm{int}} \to 0$, and $\tau_1 >> \tau_2 + \tau_3$, so that $\tau \sim \tau_1$. Then eq. (28) reduces to:

$$J = k_{\mathrm{int}}K_{\mathrm{a}}\{\mathrm{R}\}[\mathrm{M}]^{*} \tag{30}$$

which is the flux equation for the free ion activity model (FIAM) of metal uptake by microorganisms [1;20;29], for very low k_{int} values.

2- on the opposite, when interfacial transport (or consumption) is very fast ($k_{int} \rightarrow \infty$) compared to transport in solution, $\tau_1 \rightarrow 0$. Then $\tau = \tau_2 + \tau_3$. When, in addition, all complexes are fully labile i.e. their association and dissociation rates are very fast compared to diffusion, so that $\mu_i \rightarrow 0 \ \forall i$ (eq.(1)), then $\tau_3 = 0$, and:

$$J = \bar{D}_m \left(\frac{1}{r_0} + \frac{1}{\delta} \right) [\mathrm{M}]_t^* \tag{31}$$

This is indeed the expected equation for the flux of fully labile complexes, with the average diffusion coefficient $\bar{D}_m$ at a surface where $[\mathrm{M}]_0 << [\mathrm{M}]_t^*$, which is fulfilled when the consumption at the surface is very large.

3- When all complexes are inert, (i.e. $\mu_i = \delta$, $\forall i$, see below) and interfacial transport is very fast ($\tau_1 = 0$), then equation (28) reduces to:

$$J = D_{\mathrm{M}} \left(\frac{1}{r_0} + \frac{1}{\delta} \right) \ [\mathrm{M}]^* \tag{32}$$

which is the expected equation for the flux of free M at a surface where $[M]_0 << [M]^*$, with [M]* being fixed in the bulk solution by equilibrium with non labile complexes.

A few important aspects should be pointed out for a correct use of equation (28): any complex can be included in this equation, irrespective of its degree of lability, provided all complexes are sorted out according to the increasing value of μ_i. In the reaction layer approximation, by definition, complexes for which $\mu_i \geq \delta$ are taken as inert. They are all included in eq. (28) with $\mu_i = \delta$ and assumed not to contribute at all to the flux. It has been shown[16] that a negative error of 0 –24 % is thus incurred on each of these contributions, depending on their actual value of μ_i/δ. This error usually leads to a negligible error on the overall flux when mixtures

of labile, semi-labile and inert complexes are treated. $\tau_2 + \tau_3$ represents a "resistance" to the transport, due to diffusion-reaction processes, and τ_3 can be seen as a term which corrects τ_2 for the non fully labile complexes. Equations (31) and (32) give respectively the maximum and minimum possible fluxes computed by eqs (28) and (29) (with $\tau_1 = 0$) and can thus serve for validation.

2.2 Flux at a planar consuming surface.

The uptake flux at a planar consuming surface in a stirred medium, with constant value of the diffusion layer thickness, δ, is readily obtained from the general flux equation written as eq. (19), with the condition $r_0 >> \delta \geq \mu_i \ \forall i$. Under this condition, in eq. (19), each term of the type:

$$\frac{r_0^2}{\overline{\overline{D}}_{i-1}\alpha_{i-1}}\left(\frac{1}{r_0+\mu_{i-1}}-\frac{1}{r_0+\mu_i}\right) \tag{33}$$

can be simplified by considering that the parenthesis tends to $(\mu_i - \mu_{i-1})/r_0^2$. Rearranging as in eqs (28)-(29) gives

$$J = \frac{[\mathrm{M}]_t^*/\alpha_m}{\tau'} \tag{34}$$

$$\tau' = \underbrace{\frac{1}{k_{\mathrm{int}}K_a\{\mathrm{R}\}}}_{\tau_1'} + \underbrace{\frac{\delta}{\overline{D}_m\alpha_m}}_{\tau_2'} + \underbrace{\sum_{i=1}^{m}\mu_i\left(\frac{1}{\overline{D}_{i-1}\alpha_{i-1}}-\frac{1}{\overline{D}_i\alpha_i}\right)}_{\tau_3'} \tag{35}$$

with $\overline{D}_0\,\alpha_0 = D_{\mathrm{M}}$. Thus eqs (34)-(35) are just a limiting case of eq. (28)-(29) for the case of planar diffusion. τ_1', τ_2' and τ_3' are the equivalents of τ_1, τ_2 and τ_3 for diffusion at spherical surfaces, and lead to similar limiting equations for:

$\tau_1' >> \tau_2' + \tau_3'$:

$$J = k_{\mathrm{int}}K_a\{\mathrm{R}\}[\mathrm{M}]^* \tag{36}$$

$\tau_2' >> \tau_1'$, and fully labile complexes ($\mu_i \to 0 \ \forall i$, hence $\tau'_3 \to 0$):

$$J = \bar{D}_m \left[\mathrm{M}\right]_t^* / \delta \tag{37}$$

$\tau_1' << \tau_2' + \tau_3'$ and inert complexes ($\mu_i = \delta \ \forall i$) :

$$J = D_\mathrm{M} \left[\mathrm{M}\right]^* / \delta \tag{38}$$

Note that for planar diffusion, the surface area of diffusion is independent of the distance , x, from the consuming surface, so that:

$$J = J_{\mathrm{int}} = J_0 = J_{\mu_1} = J_{\mu_2} \tag{39}$$

where J_0, J_{μ_1} and J_{μ_2} are the fluxes in solution, at the distance $x = 0$, $x = \mu_1$ and $x = \mu_2$ respectively. Their expressions as well as eqs (34)-(35) can also be obtained by a derivation similar to that given in sec. 2.1, applied to planar surfaces. We highlight that eqn. (1) is applicable to both planar and spherical geometry under semi-infinite diffusion [22].

2.3. Individual contribution of each complex to the overall flux

In a complicated system including many complexes, it is often useful to know the contribution of each complex, $\mathrm{M}^i\mathrm{L}_k$, to the overall flux. It can be evaluated from the degree of lability of that complex, ${}^i\xi$, defined in [22;23] as:

$${}^i\xi = \frac{J^{\mathrm{complex}}_{\mathrm{M}^i\mathrm{L}_k}}{J^{\mathrm{dif}}_{\mathrm{M}^i\mathrm{L}_k}} = \frac{\left(1 - \dfrac{[\mathrm{M}^i\mathrm{L}_k]_0}{[\mathrm{M}^i\mathrm{L}_k]^*}\right)}{\left(1 - \dfrac{[\mathrm{M}]_0}{[\mathrm{M}]^*}\right)} \tag{40}$$

where the subscripts $_0$ and the superscript * indicate the concentrations at the consuming surface and in the bulk solution respectively. $J^{\mathrm{complex}}_{\mathrm{M}^i\mathrm{L}_k}$ is the flux due to $\mathrm{M}^i\mathrm{L}_k$, controlled both

Published in Phys.Chem.Chem.Phys 2007, vol 9, p 2844-2855
DOI: 10.1039/b700913e

by chemical and diffusion processes. $J^{\mathrm{dif}}_{\mathrm{M}^{i}\mathrm{L}_k}$ is the corresponding flux which would be obtained if the complex was fully labile. The general equation for this flux is:

$$J^{\mathrm{dif}}_{\mathrm{M}^{i}\mathrm{L}_k} = D_{\mathrm{M}^{i}\mathrm{L}_k}\left([\mathrm{M}^{i}\mathrm{L}_k]^{*} - {}^{i}\beta_k[{}^{i}\mathrm{L}]^{k}[\mathrm{M}]_0\right)\left(\frac{1}{r_0}+\frac{1}{\delta}\right) \tag{41}$$

$J^{\mathrm{complex}}_{\mathrm{M}^{i}\mathrm{L}_k}$ and the contribution to the overall flux, $J^{\mathrm{complex}}_{\mathrm{M}^{i}\mathrm{L}_k}/J_{r_0}$ are readily computed by combining (40) and (41), provided the surface concentrations of $\mathrm{M}^{i}\mathrm{L}_k$ and M are known. $[\mathrm{M}]_0$ can be obtained from eqn (3) with $J_{\mathrm{int}} = J_{r_0} = k_{\mathrm{int}}K_{\mathrm{a}}\{\mathrm{R}\}[\mathrm{M}]_0$. In addition, for the complexes with the ligand *i* (and the reaction layer μ_i), $[\mathrm{M}^{i}\mathrm{L}_k]_0$ is given by

$$[\mathrm{M}^{i}\mathrm{L}_k]_0 = [\mathrm{M}^{i}\mathrm{L}_k]_{\mu_i} = {}^{i}\beta_k[{}^{i}\mathrm{L}]^{k}[\mathrm{M}]_{\mu_i} \quad \forall k \tag{42}$$

and the value of $[\mathrm{M}]_{\mu_i}$, at each distance $r = r_0 + \mu_{\mathrm{I}}$, is obtained from the generalized eq. (13) combined with $F = J_{r_0}4\pi r_0^2$:

$$[\mathrm{M}]_{\mu_i} = [\mathrm{M}]_{\mu_{i-1}} + \frac{J_{r_0}r_0^2\left(\dfrac{1}{r_0+\mu_{i-1}} - \dfrac{1}{r_0+\mu_i}\right)}{D_{\mathrm{M}} + \displaystyle\sum_{j=0}^{i-1}\sum_{k=1}^{n_j} D_{\mathrm{M}^{j}\mathrm{L}_k}\ {}^{j}\beta_k\ \ [{}^{j}\mathrm{L}]^{k}} \tag{43}$$

with $\mu_0 = 0$ and ${}^{0}\beta_k = 0$.
Thus, by combining eqs (40) - (42) one gets:

$$\frac{J^{\mathrm{complex}}_{\mathrm{M}^{i}\mathrm{L}_k}}{J_{r_0}} = \frac{D_{\mathrm{M}^{i}\mathrm{L}_k}[\mathrm{M}^{i}\mathrm{L}_k]^{*}}{J_{r_0}}\left(1-\frac{[\mathrm{M}]_{\mu_i}}{[\mathrm{M}]^{*}}\right)\left(\frac{1}{r_0}+\frac{1}{\delta}\right) \tag{44}$$

For planar diffusion, the flux, $J_0 = k_{\mathrm{int}}K_{\mathrm{a}}\ \{\mathrm{R}\}[\mathrm{M}]_0$, at the consuming surface (x=0), replaces J_{r_0} in eq. (44) and $[\mathrm{M}]_{\mu_i}$ is obtained from eq. (43), with $r_0 >> \mu_{\mathrm{I}}$:

$$[\mathrm{M}]_0 = \frac{J_0}{k_{\mathrm{int}}K_{\mathrm{a}}\{R\}} \tag{45}$$

Published in Phys.Chem.Chem.Phys 2007, vol 9, p 2844-2855
DOI: 10.1039/b700913e

$$[\mathrm{M}]_{\mu_i} = [\mathrm{M}]_{\mu_{i-1}} + \frac{J_0\left(\mu_i - \mu_{i-1}\right)}{D_\mathrm{M} + \sum_{j=0}^{i-1}\sum_{k=1}^{n_j} D_{\mathrm{M}^j\mathrm{L}_k}\ {}^j\beta_k\,[{}^j\mathrm{L}]^k} \tag{46}$$

with $\mu_0 = 0$ and ${}^0\beta_k = 0$

3. Computational conditions

Below, the flux equations are tested systematically for 1/1 complexes, under the condition ${}^iK[{}^i\mathrm{L}]^* = [\mathrm{M}^i\mathrm{L}]^*/[\mathrm{M}]^* >> 1$ and for spherical diffusion. It has been checked, however, that the results given by equations (41)-(43) corresponding to conditions of planar diffusion, are the same as those given either by eq (28)-(29) with $r_0 >> \delta$, or by rigorous calculations using a code based on Lattice Boltzmann numerical simulation [21;27]. This paper compares the results of (28)-(29) for the approximate solution (RLA) of the flux, J_{r_0}, to a rigorous solution (RS), in excess of ligand. The latter is computed from expressions given in Appendix B, by using a previously published methodology[20;22], with three main differences: i) the (spherical) diffusion domain is finite, ii) there is an internalisation process at the surface, expressed by eq. (3), and iii) individual flux of each complex species is available. The difference between the approximated flux (J_{RLA}) and the rigorous one (J_{RS}), is computed in the form of a relative error defined as:

$$\varepsilon = \frac{J_{\mathrm{RLA}} - J_{\mathrm{RS}}}{J_{\mathrm{RS}}} \tag{47}$$

As mentioned above, the value of ε is mainly a measure of the coupling between the various chemical reactions, since J_{RLA} mostly neglects this coupling. For this reason, the influence of the chemical kinetics of the complexes is the main factor studied below. Thus the condition $\tau_1 << \tau_2 + \tau_3$ will be used in all cases. This implies that the internalisation process (J_{int} ;eq (3)) is not a rate limiting process and thus $[\mathrm{M}]_0 << [\mathrm{M}]^*$. In the context of environmental systems, the above condition implies that the computed flux will be the maximum possible flux of

Published in Phys.Chem.Chem.Phys 2007, vol 9, p 2844-2855
DOI: 10.1039/b700913e

metal towards the consuming (e.g. microorganism or sensor) surface, i.e. the flux controlled by diffusion/reactions occurring in the external medium.

A number of factors may influence the flux of a given semi-labile complex (K, k_a, k_d, D, δ, [L], see Fig.1). When mixtures of complexes are studied, the number of such factors becomes exceedingly high and makes difficult any systematic comparison. To overcome this problem, we have characterized each complex M^iL by two "combination" parameters: its reaction layer thickness, μ_i , and its lability index, $\mathcal{L}_i$. For spherical diffusion and 1/1 complexes, this latter is given by [8]:

$$\mathcal{L}_i = \frac{r_0 D_M \sqrt{{}^i k_d \left(1 + \frac{D_{M^iL}}{D_M} {}^iK[{}^iL]\right)}}{D_{M^iL}^{3/2} {}^iK[{}^iL]} \quad (48)$$

The relationship between $\mathcal{L}_i$ and μ_i is simple under the condition, $\frac{D_{M^iL}}{D_M} {}^iK[{}^iL] >> 1$ which is usually valid for all complexes in significant proportion in the test medium. Under this condition, eq. (48) simplifies to:

$$\mathcal{L}_i = \frac{r_0}{D_{M^iL}} \sqrt{\frac{D_M {}^i k_d}{{}^iK[{}^iL]}} = \frac{r_0 {}^i k_d}{D_{M^iL}} \mu_i \quad (49)$$

When $\mathcal{L}_i >> 1$, the formation/dissociation rates of the complex are very large compared to the diffusion rate. The complex can, thus, be fully dissociated and its metal ion fully consumed at an interface with fast transfer rate (large k_{int} ; $[M]_0 << [M]^*$). When $\mathcal{L}_i << 1$, the complex is non labile and does not contribute significantly to the flux. As shown by eq. (48), $\mathcal{L}_i$ not only depends on the chemical rate constants of the complex, but also on its thermodynamic

stability, its diffusion coefficient as well as the geometry of diffusion (r_0). On the other hand, μ_i (eq. (1)) only depends on the formation rate of the complex:

For each ligand *i*, μ_i was varied by keeping ${}^{i}k_a$ constant and varying [^{i}L]. In each case, the value of the lability index, $\mathcal{L}_i$, was imposed independently by varying the value of ${}^{i}K$, with ${}^{i}k_d$ being found from ${}^{i}K = {}^{i}k_a/{}^{i}k_d$. Solutions containing one, two and up to 15 ligands have been tested. The values (or range of values) of the parameters used for the computations below are given in Table 1.

4. Results

4.1. Solutions containing one ligand and two ligands with equal $\mathcal{L}$ values.

For a single ligand, L, ε was found to be smaller than 1% in the broad ranges of μ and $\mathcal{L}$ values tested, covering complex labilities from fully labile to fully non labile. This observation is consistent with the validity of eqn. (1) for the computation of the reaction layer under spherical diffusion conditions [17]. Differences between J_{RLA} and J_{RS} are significant only when μ is close to δ. This error is negative and its absolute value decreases when the ratio δ/r_0 increases. As an example, for the particular case $r_0/\delta = 0.15$, the maximum negative value of ε is around -21% for $\mu = \delta$ but ε falls to < –3% for $\mu/\delta < 0.25$.

In presence of 2 ligands, ^{1}L and ^{2}L, ε was determined by varying μ_1 over several orders of magnitudes, for various values of μ_2, by first using the condition $\mathcal{L}_1 = \mathcal{L}_2$. The value of δ was always kept much larger than μ_1 and μ_2 in order to study only the effect of synergy between ligands and avoid any finite diffusion effects. The results are shown in Figs 2 and 3a-

Published in Phys.Chem.Chem.Phys 2007, vol 9, p 2844-2855
DOI: 10.1039/b700913e

c. Figure 2 is a 3D graph for $\mathcal{L}_1 = \mathcal{L}_2 = 0.1$. Fig. 3a-c are similar results in 2D, for $\mathcal{L}_1 = \mathcal{L}_2 =$ 0.01, 1.0 and 10.0 respectively.

Figures 2-3 show that in most of the (μ_1,μ_2) domain, ε is negligible, below 5% . Only when $\mu_1 = \mu_2$, ε passes through a sharp negative maximum which corresponds to $J_{RLA} < J_{RS}$. This maximum error never exceeds 30% and decreases rapidly for $\mathcal{L}_1 = \mathcal{L}_2 > 1.0$, as shown in Fig. 4. The cause of this negative difference is treated in the discussion section. For applications to environmental systems, the major result of Figs 2-3 is that, when the lability indices of the complexes are the same, the values of J_{RLA} are correct unless the μ values of the complexes are equal, which is unlikely or exceptional in a natural system. The error is ~ -10% when $\Delta\log\mu = \log\mu_1 - \log\mu_2 = \pm 0.3$, and ~ -5% for $\Delta\log\mu = \pm 0.5$

4.2. Solution containing two ligands with different $\mathcal{L}$ values

Sets of curves with various values of $\mathcal{L}_1$ and $\mathcal{L}_2$ (such that $\mathcal{L}_1 \neq \mathcal{L}_2$) have been computed, by using the conditions given in Table 1. Figures 5a-b show that the peak of negative difference, found for $\mu_1 = \mu_2$, under the condition $\mathcal{L}_1 = \mathcal{L}_2$ (Fig. 2-3), is still present for $\mathcal{L}_1 \neq \mathcal{L}_2$, although sometimes quite small. In addition, a positive difference is found for $\mu_1 >> \mu_2$, which corresponds to RLA computed fluxes larger than the exact fluxes. The amplitude of this positive error varies from very small ones (Fig. 5b) to large ones (Fig. 5a) depending on $\mathcal{L}$ values. By comparing a large number set of curves, it was found that the maximum amplitude of this error, ε, only depends on the ratio $\mathcal{L}_2/\mathcal{L}_1$ and not on the individual values of

$\mathcal{L}_1$ or $\mathcal{L}_2$ (Fig. 6). Similarly, it was found that the position of the maximum positive error in the domain (μ_1, μ_2), denoted as $\dot{\mu}_i$, also depends on the ratio $\mathcal{L}_2/\mathcal{L}_1$ (Fig. 7).

4.3. Solutions containing more than 2 ligands.

Systematic studies of the differences between RLA and RS are difficult to perform for a large number of ligands, since the number of μ and $\mathcal{L}$ combinations becomes exceedingly large. It is possible however to consider the case where the labilities of all ligands are the same. This is shown in Fig. 8, where successively 2, 3, 4, up to 15 ligands have been considered, with $\mathcal{L}$ = 1 for all of them. For 2 ligands, μ_1 has been fixed at $\mu_1 = 5\times10^{-8}$m and μ_2 was varied up to 10^{-6}m. The peak of negative error for two ligands (symbol● in Fig. 8), already shown in Figs 2-3, is also included. For 3 ligands, μ_1 and μ_2 were fixed at 5×10^{-8} m, and μ_3 was varied. Fig. 8 shows that when the formation rate of M^3L is faster than those of M^1L and M^2L ($\mu_3 < 5\times10^{-8}$ m) the overall error is weak or even negligible. For $\mu_3 > 5\times10^{-8}$m, the error due to M^3L is negligible, but the error due to M^1L and M^2L (for which $\mu_1 = \mu_2 = 5\times10^{-8}$m) is non negligible and this latter controls the overall error. When $\mu_3 = 5\times10^{-8}$ m, M^3L contributes an additional error to that produced by M^1L and M^2L, but to a lesser extend. The same trend is observed for larger number of ligands (Fig. 8).

Figure 9 shows how the maximum negative error of Fig. 8 (when all μ values are equal) varies in a less than linear manner with the number of ligands. The figure suggests that this maximum error tends to a limiting value of 70-80%, for ligand numbers larger than 15 (symbols●). It must be emphasized that this curve corresponds to the maximum possible difference between RLA and RS computations, when all values of μ are equal. It enables to

obtain a feeling of this difference when many ligands are present. But in practical applications, it is a non realistic case, since μ values of the various ligands are usually different from each others, so that the overall difference between J_{RLA} and J_{RS} is much smaller.

Evaluations of ε, in case of many ligands whose μ values are different but $\mathcal{L}$ values are the same, have been performed in the following cases (Fig. 9):

- 2 to 10 ligands with μ values in between 4×10^{-9} and 6.7×10^{-9} m with constant spacing of $\Delta\mu = 3\times10^{-10}$ m (symbol □ in Fig. 9).
- 2 to 4 ligands with μ values in between 4×10^{-9} and 7×10^{-9} m with constant spacing of $\Delta\mu = 10^{-9}$ m (symbol ▲ in Fig. 9).

Figure 9 shows that the overall maximum error decreases quickly when $\Delta\mu/\bar{\mu}$ increases, where $\bar{\mu}$ is the average value of the explored range of μ (5.5×10^{-9} m in the two cases above). The maximum error is equal to ~ -60% and - 20 % for $\Delta\mu/\bar{\mu}$ = 0.055 and 0.18 respectively.

Non systematic tests have suggested that when $\mathcal{L}$ values are different from each other, the maximum positive difference between RLA and RS computations is still determined by the maximum value of the $\mathcal{L}$ ratio in the system, according to Fig. 6, and is independent from the number of complexes.

Published in Phys.Chem.Chem.Phys 2007, vol 9, p 2844-2855
DOI: 10.1039/b700913e

5. Discussion

In general, the causes of differences between RS and RLA are attributed to both mathematical limitations due to conceptual approximations and to the coupling of kinetics of the various complexes which is neglected in the reaction layer approximation.

A mathematical difficulty in the rigorous solution

The precise condition $\mu_1 = \mu_2$ and $\mathcal{L}_1 = \mathcal{L}_2$, which also implies ${}^1k_d = {}^2k_d$, cannot be directly dealt with the general equations of the RS solution proposed in Appendix B, because it leads to a system of linear equations with a singular matrix. In such event, a previous very simple combination of the variables (as described in Appendix D) allows to prevent the mathematical difficulty and enables to simply apply the procedure of Appendix B. This condition is considered in the code FLUXY, which always tests it and provides a warning. In the computation of sections 4.1, the parameters were chosen in such a way that the relative difference between μ_1 and μ_2 be ≥ 0.0001, which is sufficient to avoid the above singularity problem.

Interpretation of the negative difference between RS and RLA:

Figure 10 shows the changes of the fluxes at the interface, computed by RS and RLA, when μ_1 increases (e.g. due to a change in $[{}^1L]$), by keeping μ_2 constant. The following observations can be made:

i) when μ_1 and μ_2 are sufficiently different from each other (typically a ratio of about 2, indicated by the vertical dashed lines) the relative differences between the two fluxes is very small.

ii) When μ_1 and μ_2 approach each other, the difference increases gradually. This is linked to a physical coupling between M^1L and M^2L, as detailed in point b) below.

Published in Phys.Chem.Chem.Phys 2007, vol 9, p 2844-2855
DOI: 10.1039/b700913e

iii) At $\mu_1 = \mu_2$ there is an abrupt change in the slope of the RLA curve in fig. 10, which is due to a mathematical discontinuity in RLA equation, as explained in point a) below.

a) Conceptual and mathematical discontinuity

Observation iii) corresponds to the sharp peaks seen in Figs. 2, 3 and 5. This discontinuity is produced by the algorithm of the RLA equation, with requires to sort out the reaction layer thicknesses in the increasing order of μ_i values. For instance, let us consider the case of Fig. 10 where μ_2 is constant and μ_1 increases from $\mu_1 < \mu_2$ to $\mu_1 > \mu_2$. During the continuous scan of μ_1, an abrupt change arises in the order of μ_1 and μ_2 at $\mu_1 = \mu_2$, and correspondingly, the functionality of J with respect to μ_1 (and μ_2) in eqs. (29) or (34) changes. This explains the sharp peak shape in figs 2, 3 and 5. In general, in either the spherical or planar case, the absolute value of the error of each of the two previous equations increases when the variable μ_1 tends to the fixed μ_2.

b) Physical interpretation of the negative difference between RS and RLA

Observation ii) about Fig. 10 is interpreted by considering that the RLA concept neglects most of the interaction (or coupling) between the various complexes (M^1L and M^2L in Figs 1 and 10). When the formation rate of one of the two complexes is much lower than that of the other, they can indeed be considered as independent from each other. However, when ${}^1k_a[{}^1L]$ and ${}^2k_a[{}^2L]$ are of the same order of magnitude, the concentration profiles of free M and the two complexes are influenced by both ligands simultaneously. Then, the reaction layer concept is still applicable, but only one reaction layer should be considered, which takes into account the formation rate of both complexes[19;32]. As shown in Appendix E, the new global (or equivalent) reaction layer thickness, which should be used in the RLA approach for two

such ligands, can be derived as $\mu_{equiv} = \sqrt{\frac{D_M}{{}^1k_a[{}^1L] + {}^2k_a[{}^2L]}}$. At $\mu_1 = \mu_2$, this simplifies to $\mu_{equiv} = \mu_1/\sqrt{2} = \mu_2/\sqrt{2}$, where μ_1 and μ_2 are the values given by eq. (1). Introducing this expression in eq. (34) and comparing with the expression of eq. (34), when the two complexes are considered as independent, enables to get the mathematical expression for ε. The general expression for *m* complexes with the same value of $\mu = \mu_1$ is (Appendix E, eq. (E-7))

$$\varepsilon = \frac{m\ {}^1K[{}^1L]\ r_0\left(\frac{1}{r_0+\mu_1} - \frac{\sqrt{m}}{r_0\sqrt{m}+\mu_1}\right)}{1 + m\ {}^1K[{}^1L] - \frac{r_0}{r_0+\delta} - \frac{r_0\, m\ {}^1K[{}^1L]}{r_0+\mu_1}} \qquad (50)$$

This equation indeed explains quantitatively the negative difference between RLA and RS, as it can be seen by the full line in Fig. 4 (case of $m = 2$ and varying values of $\mathcal{L}_1 = \mathcal{L}_2$), and Fig. 9 ($m = 2$ to 15, with equal μ values and equal $\mathcal{L}$ values).

Thus, the negative error is mainly linked to the assumption in RLA that the behaviour of complexes are independent from each other, and that each given complex has a specific reaction layer thickness. This approximation is very good when the μ values differ by a factor of at least 2, but not when they are closer to each other. Effects ii) and iii) apply simultaneously. They are both coherent with the negative difference between the results of RLA and RS in § 4.1 and 4.2, for $\mu_1 = \mu_2$, irrespective of the values of $\mathcal{L}$. The above explanation is also coherent with the fact that this difference decreases to 0% when both $\mathcal{L}_1$ and $\mathcal{L}_2$ are larger than 1. This is physically expected, since, for fully labile complexes, equation (28) tends to eq. (31), which is independent of the μ-value. In other words, when the

complexes are very labile, μ_1, μ_2 and μ_{equiv} are all negligible compared to r_0 and the difference between eqns. E-(1) and (E-4) vanishes. Figs 6 and 9 also suggest that the negative error accumulates, but in a less than linear manner (according to eqn. (E-7)), when the number of complexes (with the same μ and $\mathcal{L}$ values) increases.

The sharp negative error observed with one single complex, for $\mu = \delta$ (section 4.1), is explained by a mathematical discontinuity similar to that with two complexes and $\mu_1 = \mu_2$. When μ is scanned from $\mu < \delta$ to $\mu > \delta$, an abrupt changes occurs at $\mu = \delta$, since the RLA algorithm requires to impose $\mu = \delta$ for any value of μ larger than δ. For μ values close to δ, the negative error is ascribed to the fact that eqn (1) is derived for *semi-infinite* diffusion at planar or spherical interfaces whereas the case $\mu = \delta$, by definition, corresponds to a finite diffusion problem. Under such a condition, specific expressions for μ arise [19] where, as physically expected, μ is always less than δ. So, the error for cases with $\mu \sim \delta$ can be mostly ascribed to the overestimation of μ, arising from its computation by eqn (1).

Interpretation of the positive difference between RS and RLA

Under specific conditions (section 4.2), a positive difference is observed between RLA and RS computations, when $\mathcal{L}_1 \neq \mathcal{L}_2$ and $\mu_1 \neq \mu_2$. This is attributed to the simplifying assumption made in RLA, on the dynamics of M^1L and M^2L, between $r_0 + \mu_1$ and $r_0 + \mu_2$. Indeed, in this domain (Fig. 1), M^2L is supposed to be fully non labile, and in particular M cannot associate again to ^2L, whereas this is not totally true in practice[33]. Simultaneously, M^1L is supposed to be fully labile, which is also not completely correct. The net result is that the contributions of M and M^1L to the flux, in this layer, is overestimated, which leads to a positive error when the chemical rate constants are large enough. This explanation has been checked by varying the k_a values of both complexes, while keeping their ratio constant in order to also keep constant the

Published in Phys.Chem.Chem.Phys 2007, vol 9, p 2844-2855
DOI: 10.1039/b700913e

ratios μ_2/μ_1 and $\mathcal{L}_2/\mathcal{L}_1$. It is expected that at large values of ${}^1k_a$ and ${}^2k_a$, the error will become negligible, because both complexes are fully labile and under such conditions, eq. (28) tends to the rigorous form for labile complexes (eq (31)). By referring to Fig 1, this situation corresponds to the case where μ_1 and μ_2 are so small that the corresponding surfaces are compressed at the consuming surface at r_0, with $[M]_0 << [M]^*$, $[M^1L]_0 << [M^1L]^*$ and $[M^2L]_0 << [M^2L]^*$. At very low ${}^1k_a$ and ${}^2k_a$ values, both complexes are inert and eq. (28) reduces to the rigorous eq. (32). Thus again, a negligible difference between RLA and RS computations should be observed. In Fig. 1, this situation corresponds to the case where μ_1 and μ_2 are compressed at $r = r_0 + \delta$. Then only M diffuses towards the consuming surface. On the other hand, the difference between RLA and RS may be larger for intermediate values of ${}^1k_a$ and ${}^2k_a$, due to the aforementioned approximation. Figure 11 shows that such predictions are indeed observed. As expected, the maximum value of the error increases with the difference between μ_1 and μ_2. Interestingly for practical applications, this negative difference between RLA and RS, only occurs for very large k_a values, which are most often physically non realistic.

6. Conclusion

The above results show that the reaction layer approximation enables to compute the metal flux at a consuming surface, with a good accuracy, in many cases. Under a few specific conditions systematically studied in this paper, the difference between RLA and RS computation may be non negligible. In particular:

i) the negative error is significant for two complexes (> 5% with a maximum at 30%), when $\Delta\log\mu < 0.5$ and all $\mathcal{L}$ values are equal and smaller than 1. It levels off with the number of ligands.

ii) the positive error may be > 100%, for $\mathcal{L}_2/\mathcal{L}_1 > 100$ and very large k_a values. It is negligible for any ratio of lability index and μ values, when the association rate constants are smaller than 10^{12} L $mol^{-1}s^{-1}$

Such conditions for a significant positive error are rarely encountered and, even when they are fulfilled, the RLA approach may be useful to quickly provide a good order of magnitude of the flux in complicated systems. Indeed, in environmental or biological systems, the error on computed fluxes is usually controlled by the large uncertainties on the stability constants, rate constants and diffusion coefficients of the involved species.

Apart from its easy application to complicated environmental systems, the RLA leads to simple analytical equations, with direct physico-chemical meaning. It becomes then easier than with a rigorous, numerical solution, to evaluate the role of a specific complex on the overall flux. It should also be noted that presently, the RS approach is applicable only to 1/1 complexes, whereas successive complexes ML_k (k>1) can be considered with RLA when the rates of formation/dissociation of ML_k are larger than those of the 1/1 complex ML (section 2.1). As exemplified in this paper, comparison of the RLA and RS results may become a very useful tool to better understand the reaction/diffusion coupling of many simultaneous processes in a complicated system.

Acknowledgements

The Swiss National Foundation is gratefully acknowledged for its support (project n° 200020-101974/1). This work was also supported by an EU project (ECODIS, contract n° 518043-1). JG acknowledges support by the Spanish Ministry of Education and Science (DGICYT BQU2003-07587) and from the "Comissionat d'Universitats i Recerca de la Generalitat de Catalunya".

Published in Phys.Chem.Chem.Phys 2007, vol 9, p 2844-2855
DOI: 10.1039/b700913e

Table of symbols

D_M diffusion coefficient of free M

$D_{M\,{}^{i}L_k}$ diffusion coefficient of M^iL_k

$\dot{D}_i$ average diffusion coefficient of all complexes containing ligand ${}^{i}L$

$\overline{D}_i$ weighted average diffusion coefficient for complexes with ligands n° 1 to *I*

J flux at a certain position (indicated by superscript or subscript)

${}^{i}k_a$, ${}^{i}k_d$ association and dissociation rate constants of M^iL_k.

$\mathcal{L}_i$ Lability index of complex with index number *i*

${}^{i}L$ Ligand with index number *i*

m Maximum number of different types of ligands (^1L, ^2L..^mL)

[M] concentration of free M

n_j maximum number of successive complexes formed between M and ${}^{j}L$

r_0 radius of the spherical consuming surface

α_i Degree of complexation of M by ligands n° 1 to *i*

${}^{i}\beta_k$ Cumulative stability constant of M^iL_k

δ reactive-diffusion layer thickness

ε Relative difference between fluxes computed by RLA and RS approaches

μ_i reaction layer thickness of complex M^iL

[]*, $[]_0$, $[]_{ro}$ concentrations in the bulk solution, at the distance x=0 of the consuming interface (planar geometry), and at $r=r_0$ (spherical geometry).

Published in Phys.Chem.Chem.Phys 2007, vol 9, p 2844-2855
DOI: 10.1039/b700913e

Table 1

Values of the parameters used for computations

Constant parameters	
r_0	2 μm
δ	100 μm
$k_{int} K_a \{R\}$	67.5 $m \cdot s^{-1}$
${}^i k_a$	9.5×10^{10} and 2.86×10^{13} $L \cdot mol^{-1} \cdot s^{-1}$ (except in Fig. 11 where ${}^1 k_a$ varied)
$D_M = D_{M^i L_k}$	7.2×10^{-10} $m^2 \cdot s^{-1}$ ($\forall i, k$)
$[M]_t$	10^{-8} M
Variable parameters (ranges of values)	
${}^i K [{}^i L]$	10 to 10^5
$[{}^1 L]$	10^{-9} to 10^{-3} M (in a few cases down to 10^{-12} M)

Published in Phys.Chem.Chem.Phys 2007, vol 9, p 2844-2855
DOI: 10.1039/b700913e

Legends of figures

Figure 1.

Schematic reaction/diffusion processes for a system with two ligands, ^{1}L and ^{2}L and two complexes M^{1}L and M^{2}L. Schematic representations of the reaction layers, μ_1 and μ_2, and the concentration profiles of M, M^{1}L and M^{2}L, between r_0 and $r_0+\delta$. R is the complexation site at the consuming surface; k_{int} stands for the internalization rate constant. D_M and D_{M^iL} represent diffusion coefficients of M and M^{i}L; ^iK, ^ik_a and ^ik_d are the equilibrium constant and the association and dissociation rate constants of the complex.

Figure 2.

Relative difference between fluxes from RLA and RS computations (see eqn. (47)) for a 2 ligand system keeping $\mathcal{L}_1 = \mathcal{L}_2 = 0.1$ (see eq (48)). Parameters used for computation: see table 1.

Figure 3a-c

Relative difference between RLA and RS computations for a 2 ligand system and $\mathcal{L}_1 = \mathcal{L}_2 = 0.01$ (Fig. 3a), 1.0 (Fig. 3b), 10.0 (Fig. 3c). Parameters used for computation: see table 1. All values of μ are in micrometers.

Figure 4

Maximum negative error ($\mu_1=\mu_2$) as function of the commun value of the lability index. Dots are the difference between RS and RLA (eq. (34)). The full line curve is obtained from the theoretical expression for ε (See discussion, eq.(50)). Computation parameters: see Table 1.

Figure 5

Relative difference between RLA and RS computations for 2 ligand system with $\mathcal{L}_1 \neq \mathcal{L}_2$

Fig. 5a: $\mathcal{L}_1 = 0.1$, $\mathcal{L}_2 = 10.0$. Fig. 5b: $\mathcal{L}_1 = 0.01$, $\mathcal{L}_2 = 0.1$. Parameters used for computation: see table 1. All values of μ are in micrometers.

Figure 6

The maximum positive difference between RLA and RS computations, ε, as a function of the ratio between $\mathcal{L}_1$ and $\mathcal{L}_2$. The error depends only on this ratio, but not on the individual values of $\mathcal{L}$. Parameters used for computation: see Fig. 5 and Table 1

Figure 7

Position of the maximum positive difference between RLA and RS computations, in the (μ_1, μ_2) domain, as function of $\mathcal{L}$ ratio. $\dot{\mu}_i$ corresponds to the position of the maximum error, on μ_1 axis, for a given value of μ_2. Parameters used for computation: see Fig. 5 and Table 1

Figure 8

Negative error for multiligand systems. For each symbol, the μ values for all ligands except the last one, were kept the same (5×10^{-8}m), while the value of μ for the last added ligand (= μ_ℓ) was varied (see text for details). The labilities of all complexes were set equal to 1.0. Two, 3, 4, 7, 10 and 15 ligands are considered. Parameters used for computations: see table 1.

Figure 9

Maximum negative error vs. the number of ligands, whose μ values differ by various, constant, Δμ spacing (see text); (●)Δμ= 0 , (□) Δμ = 3×10^{-4} μm, (▲) Δμ= 10^{-3} μm . $\mathcal{L}$ values of all complexes =1.0. Parameters used for computations: see table 1. For Δμ = 0, the dots are the difference between RS and RLA (eq.), and the full line curve is obtained from the theoretical expression for ε (see discussion, eq.).

Figure 10

Fluxes computed by RS (dotted line, see Appendix D) and RLA using either the individual reaction layers of each complex (dashed line, eq. (29) for 2 ligands) or just one equivalent reaction layer thickness for both complexes (full line; eq. (E-4) with $K'_{\text{equiv}} = {}^1K[{}^1\text{L}] + {}^2K[{}^2\text{L}]$ and $\mu_{\text{equiv}} = \sqrt{\frac{D_{\text{M}}}{{}^1k_{\text{a}}[{}^1\text{L}] + {}^2k_{\text{a}}[{}^2\text{L}]}}$; μ_{equiv} varies due to the change of ^{1}L). Note that dotted and full line curves practically collapse. The fixed value of ${}^2k_{\text{a}}[{}^2\text{L}]$ is 2.85×10^7 which corresponds to $\mu_2 = 1.59\times10^{-8}$ m (central vertical line). Dashed vertical lines are placed at $\mu_2/2$ and $2\times\mu_2$. Parameters: ${}^1k_{\text{d}} = {}^2k_{\text{d}} = 1.5\times10^5$ s^{-1}; ${}^1k_{\text{a}} = {}^2k_{\text{a}} = 9.496\times10^7$ mol^{-1} m^3 ; [^{2}L]= 0.03 mol m^{-3} ; $r_0=5\times10^{-6}$ m; $k_{\text{int}}\,K_{\text{a}}\,\{\text{R}\}=67500$ m·s^{-1}. Other parameters as in Table 1.

Figure 11

Two ligand system: dependence of the positive difference between RLA and RS computations on ${}^1k_{\text{a}}$ for constant ${}^1k_{\text{a}}/{}^2k_{\text{a}}$, $\mathcal{L}_1/\mathcal{L}_2$ and μ_1/μ_2 ratios. $\mathcal{L}_1 = 0.01$, $\mathcal{L}_2 = 10$. $\mu_1/\mu_2 = 100$ (■), 3.1 (●). Other parameters: see table 1. The range of k_{a} values used here are required to cover the whole range of μ and $\mathcal{L}$ values. k_{a} values larger than 10^{14} M^{-1}s^{-1} are not physically realistic, but just enable to show the mathematical reason of the positive error, as discussed in the text.

Published in Phys.Chem.Chem.Phys 2007, vol 9, p 2844-2855
DOI: 10.1039/b700913e

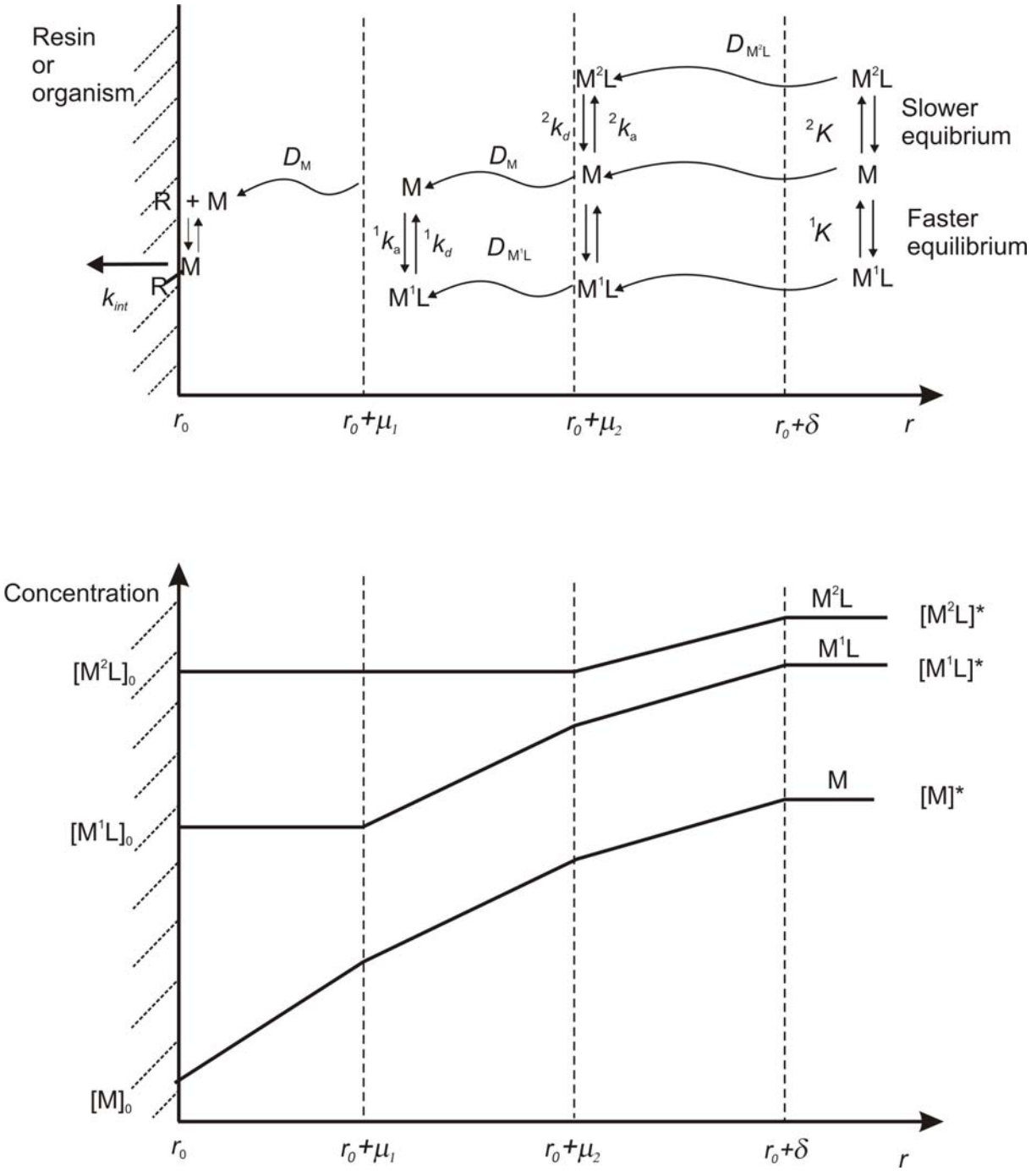

Figure 1

Published in Phys.Chem.Chem.Phys 2007, vol 9, p 2844-2855
DOI: 10.1039/b700913e

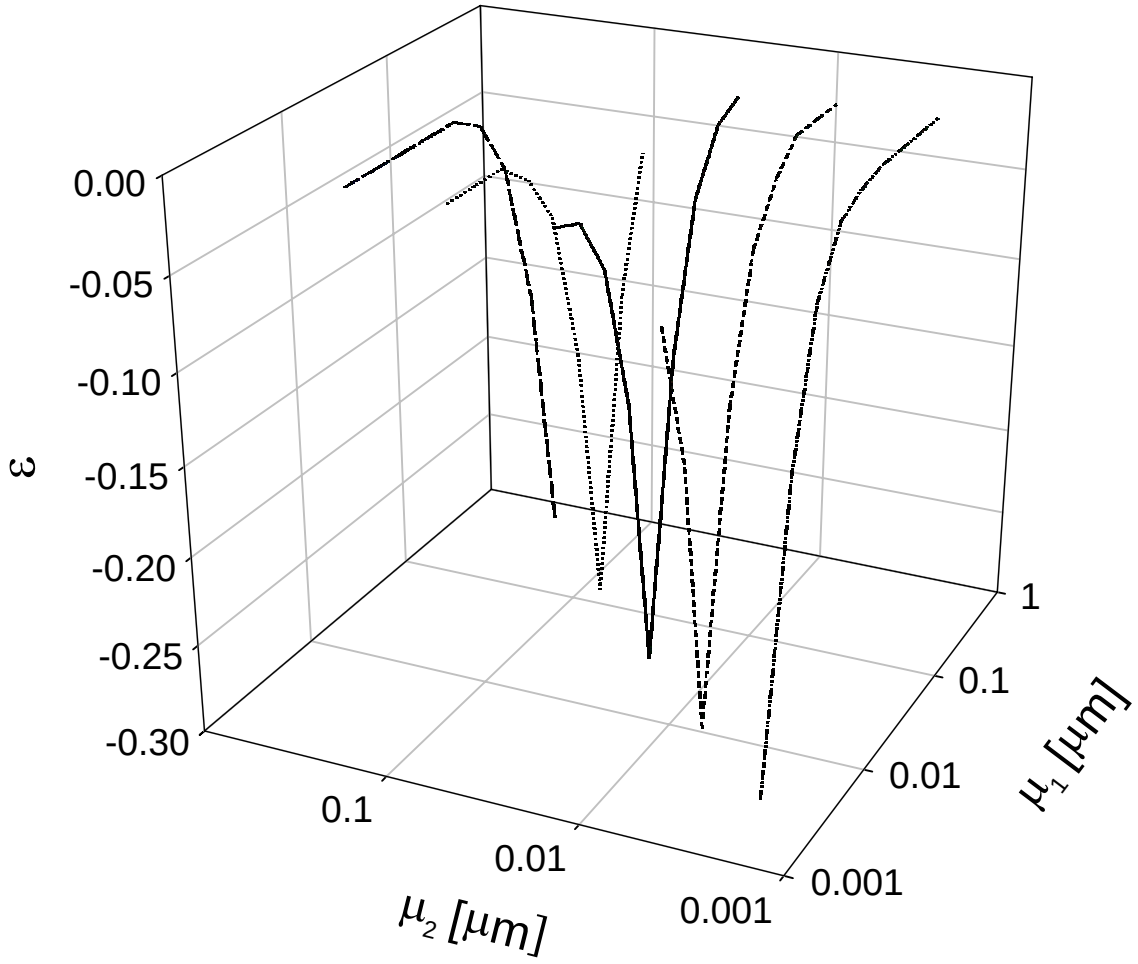

Fig. 2

Published in Phys.Chem.Chem.Phys 2007, vol 9, p 2844-2855
DOI: 10.1039/b700913e

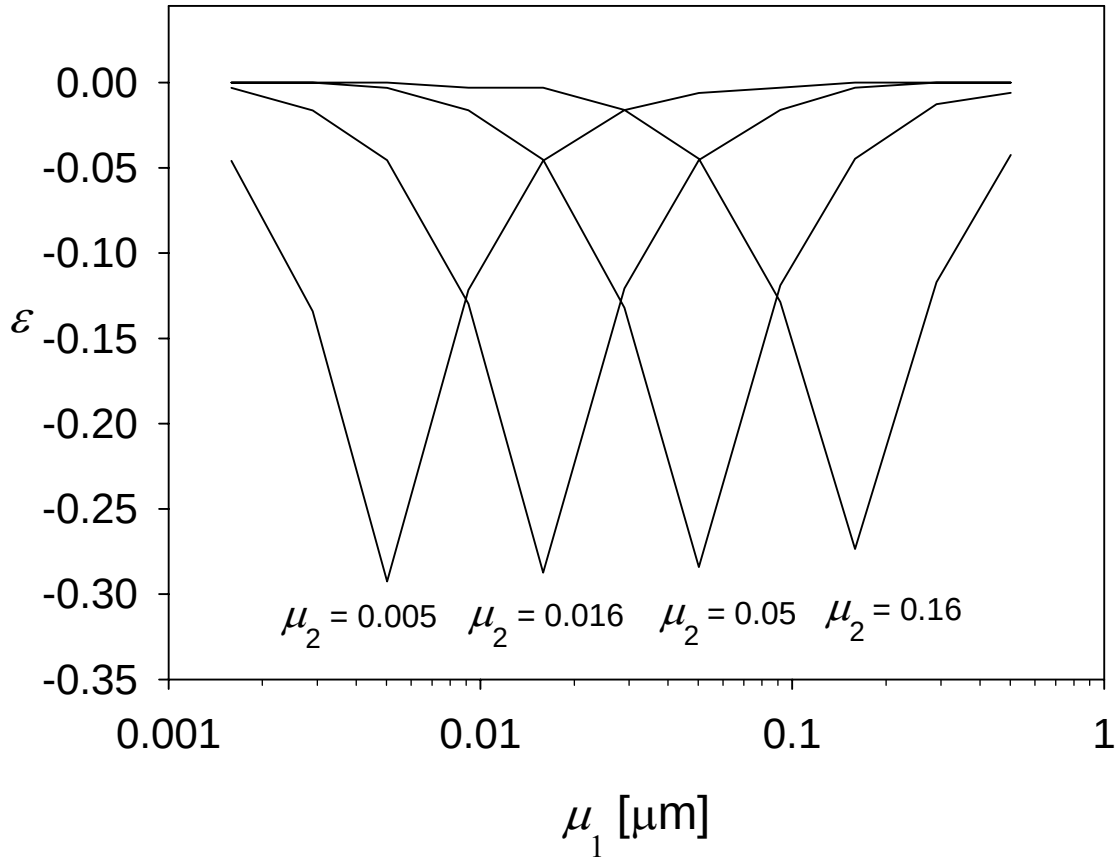

Fig. 3a.

Published in Phys.Chem.Chem.Phys 2007, vol 9, p 2844-2855
DOI: 10.1039/b700913e

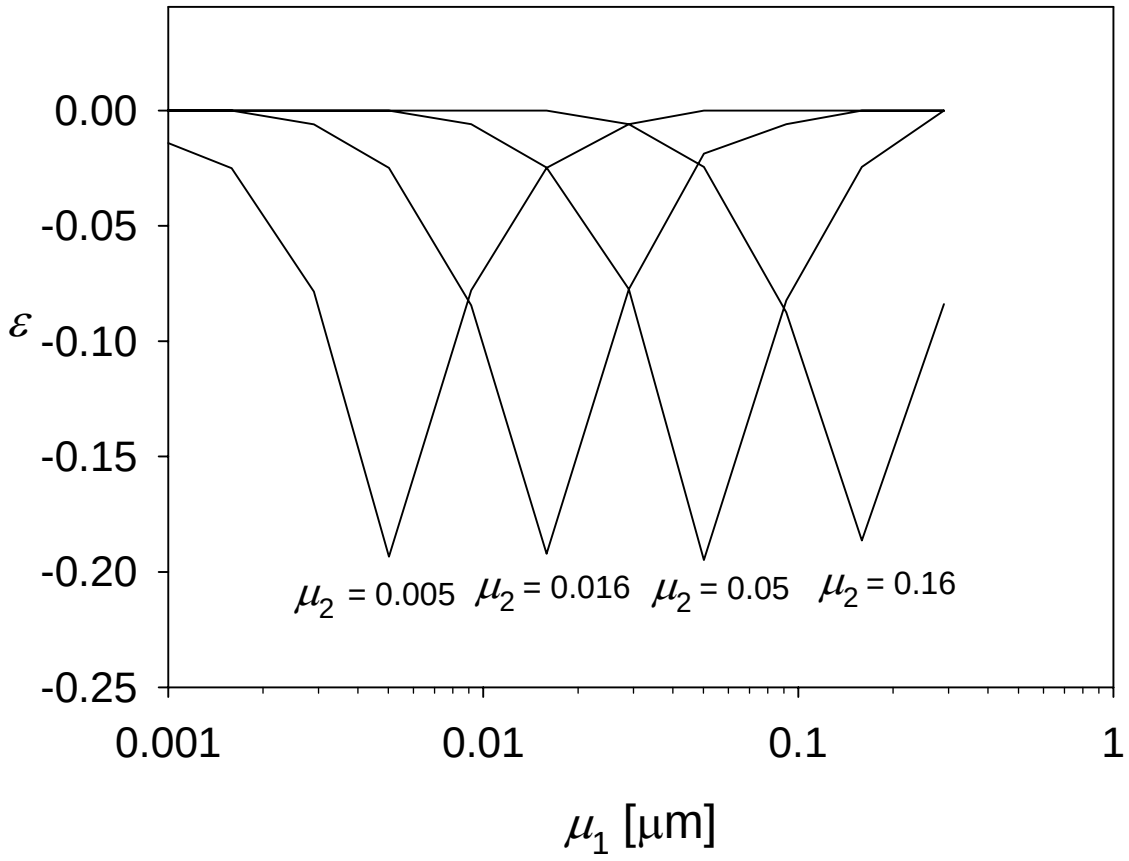

Fig. 3b.

Published in Phys.Chem.Chem.Phys 2007, vol 9, p 2844-2855
DOI: 10.1039/b700913e

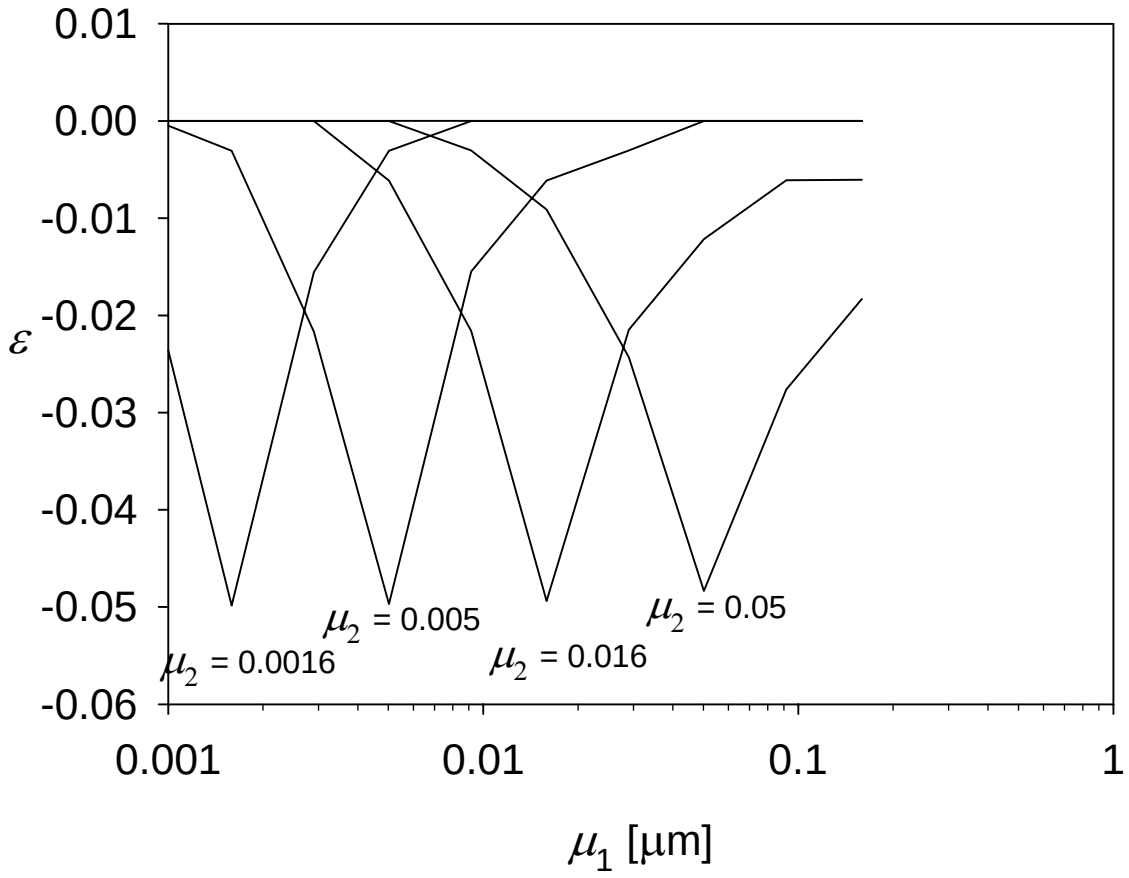

Fig. 3c.

Published in Phys.Chem.Chem.Phys 2007, vol 9, p 2844-2855
DOI: 10.1039/b700913e

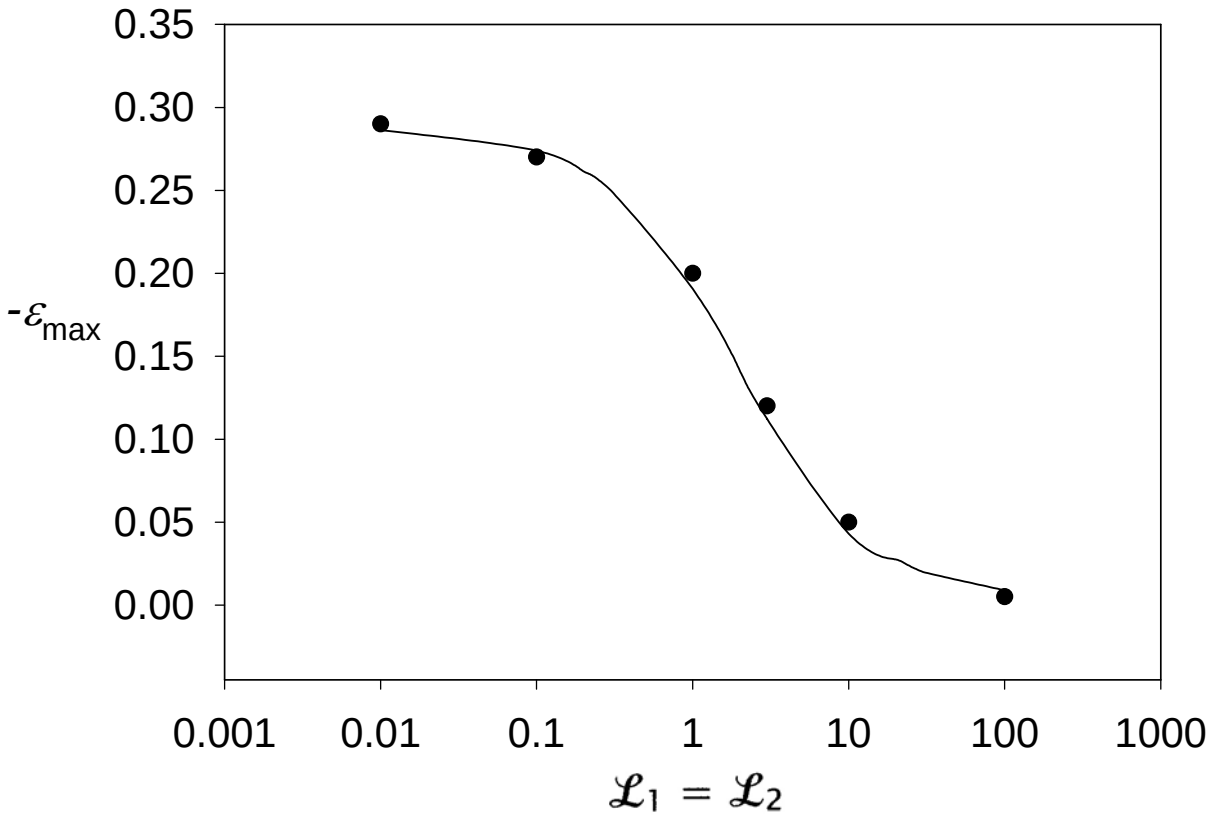

Figure 4

Published in Phys.Chem.Chem.Phys 2007, vol 9, p 2844-2855
DOI: 10.1039/b700913e

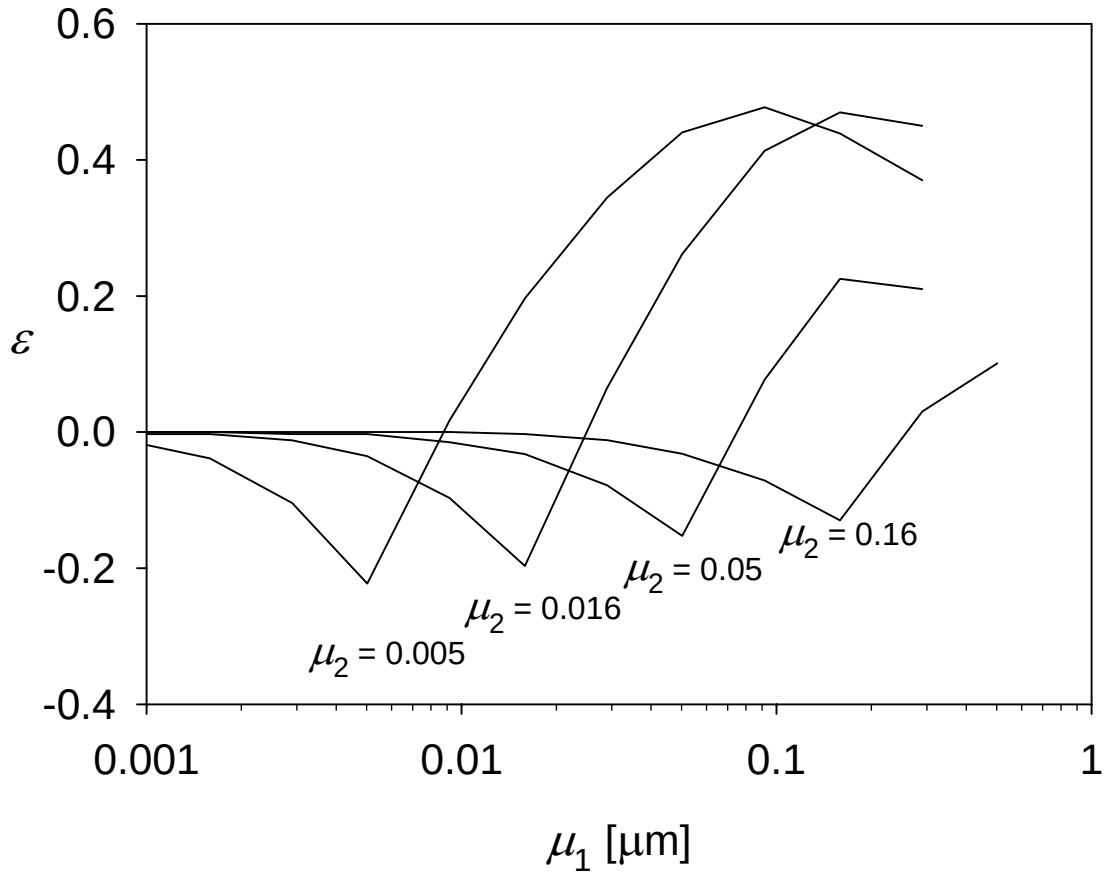

Fig. 5a.

Published in Phys.Chem.Chem.Phys 2007, vol 9, p 2844-2855
DOI: 10.1039/b700913e

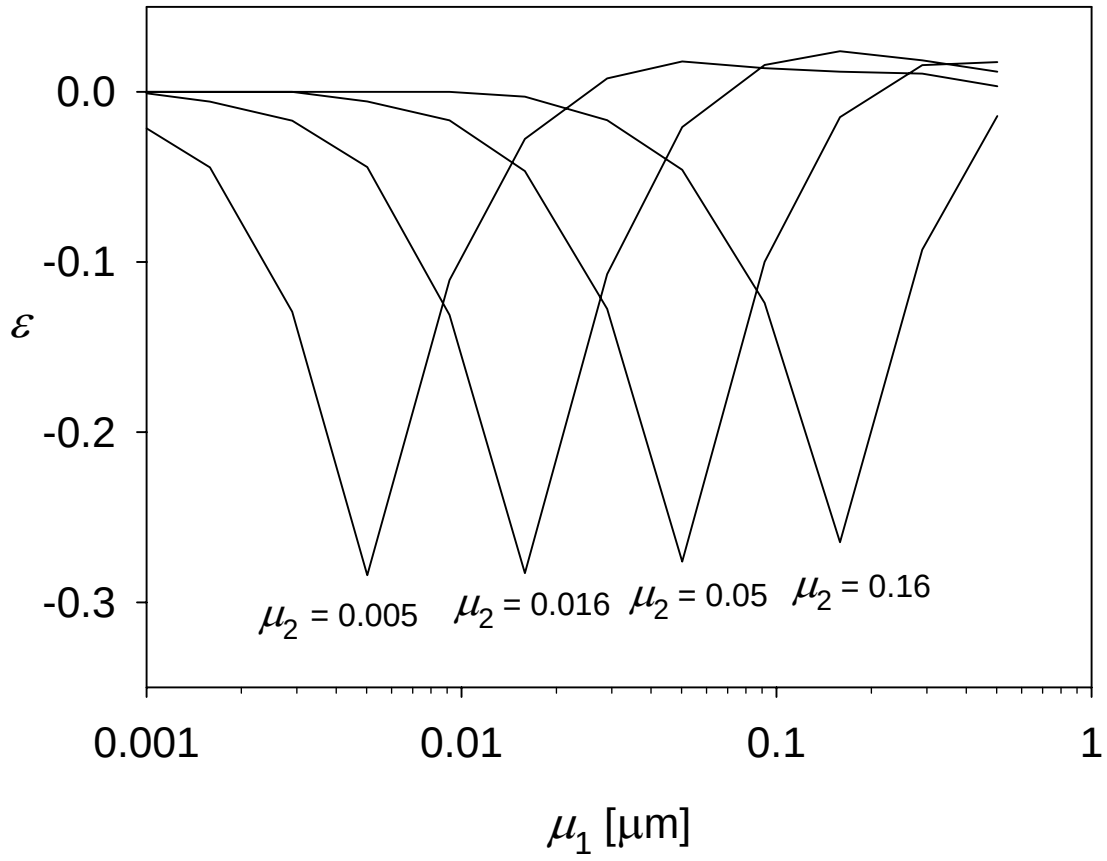

Fig. 5b.

Published in Phys.Chem.Chem.Phys 2007, vol 9, p 2844-2855
DOI: 10.1039/b700913e

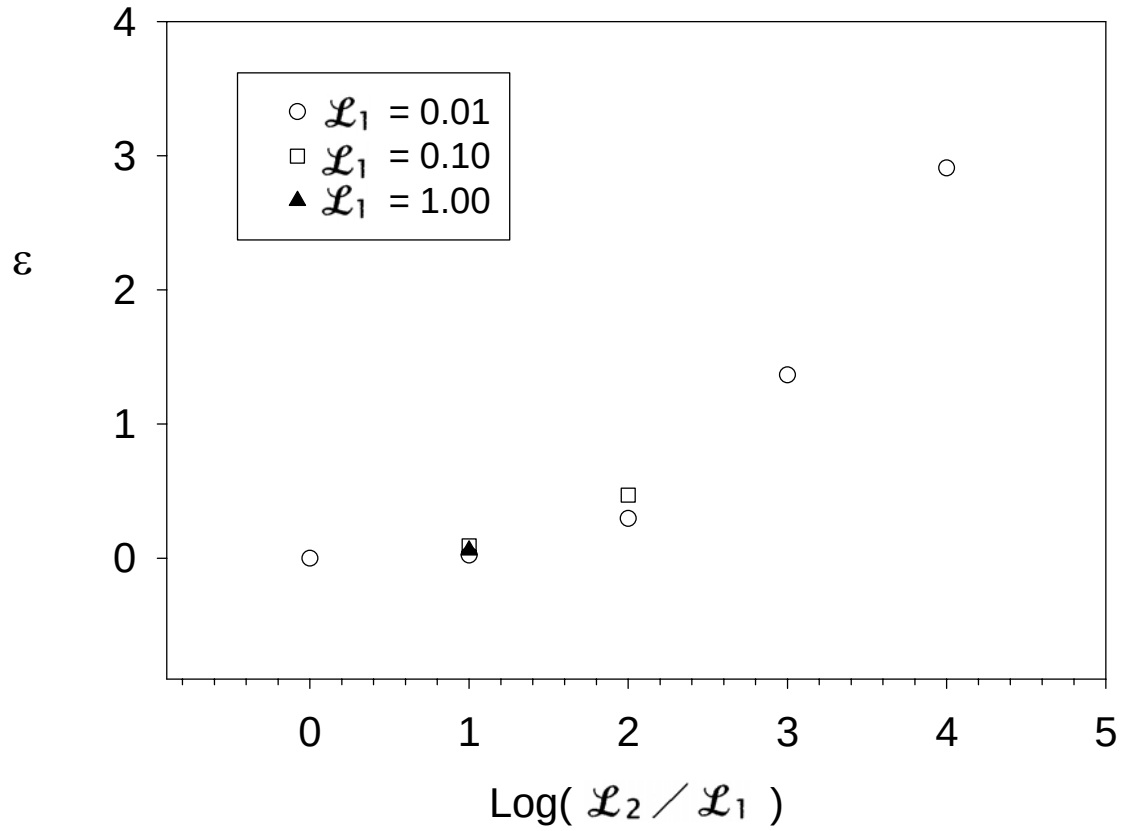

Fig. 6.

Published in Phys.Chem.Chem.Phys 2007, vol 9, p 2844-2855
DOI: 10.1039/b700913e

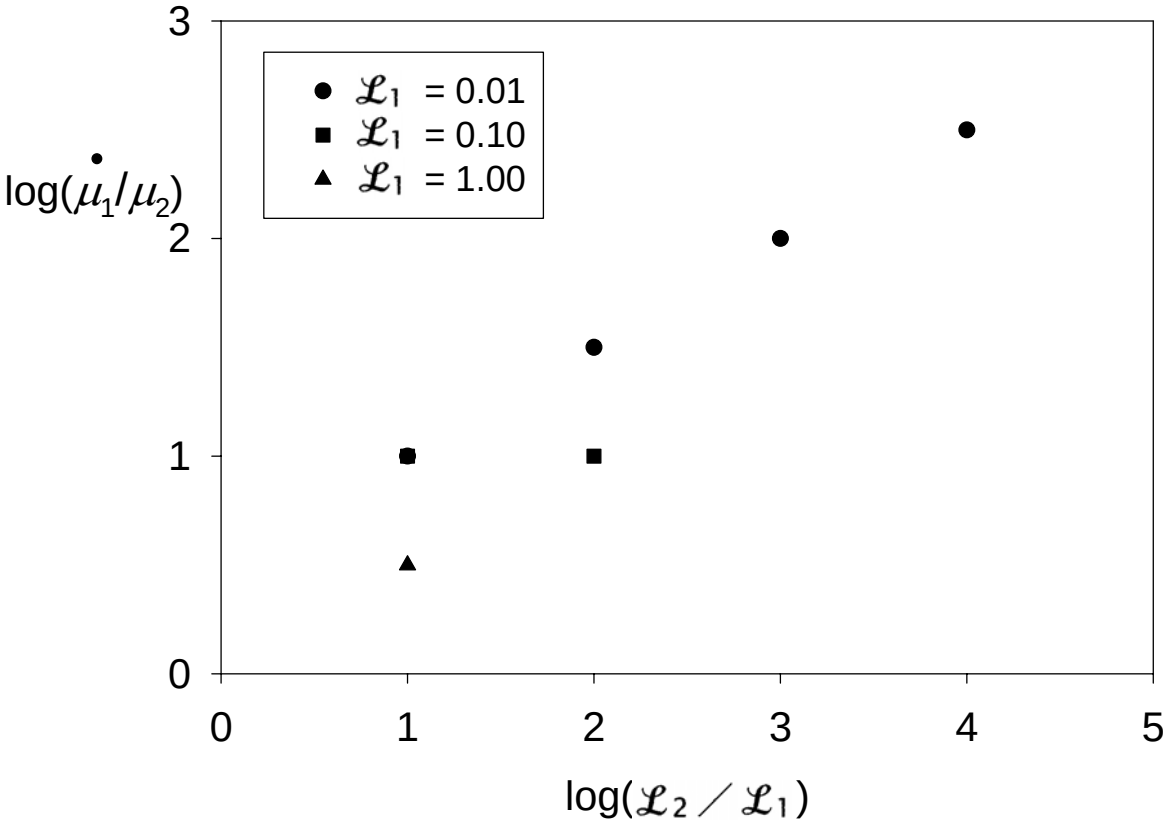

Fig. 7.

Published in Phys.Chem.Chem.Phys 2007, vol 9, p 2844-2855
DOI: 10.1039/b700913e

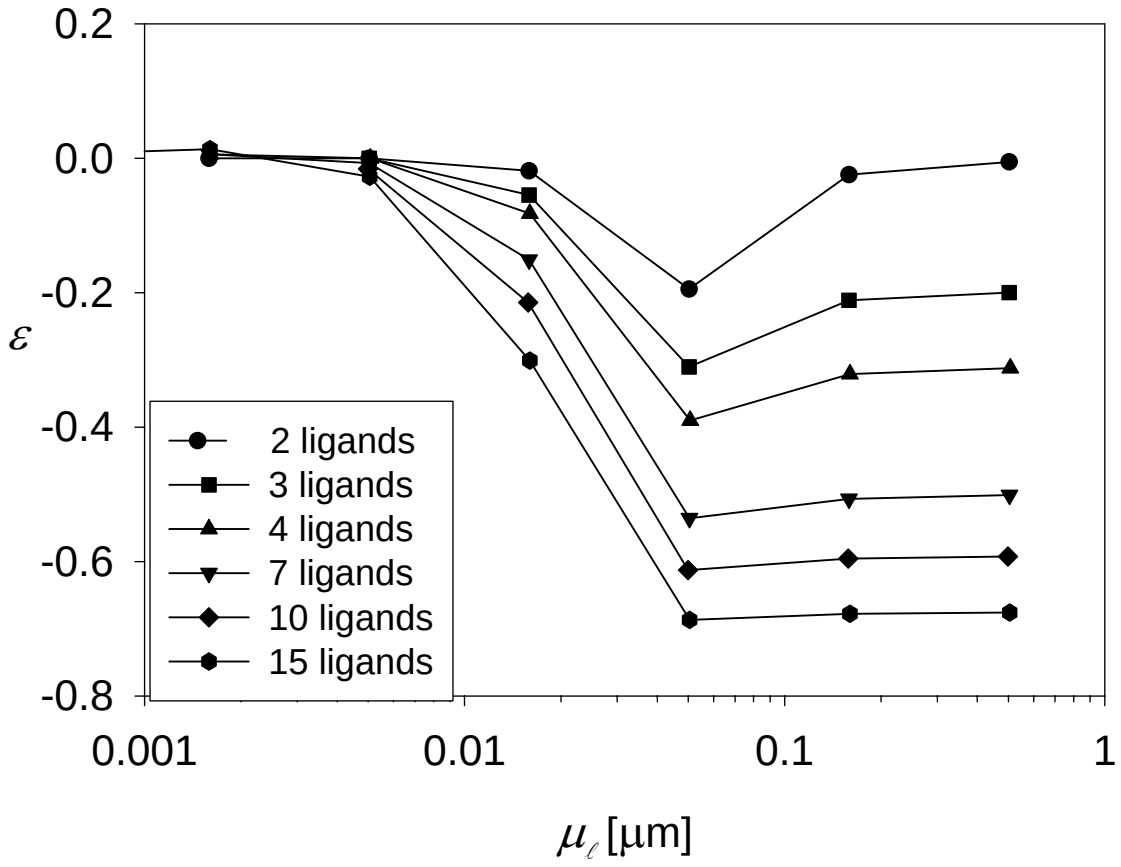

Fig. 8.

Published in Phys.Chem.Chem.Phys 2007, vol 9, p 2844-2855
DOI: 10.1039/b700913e

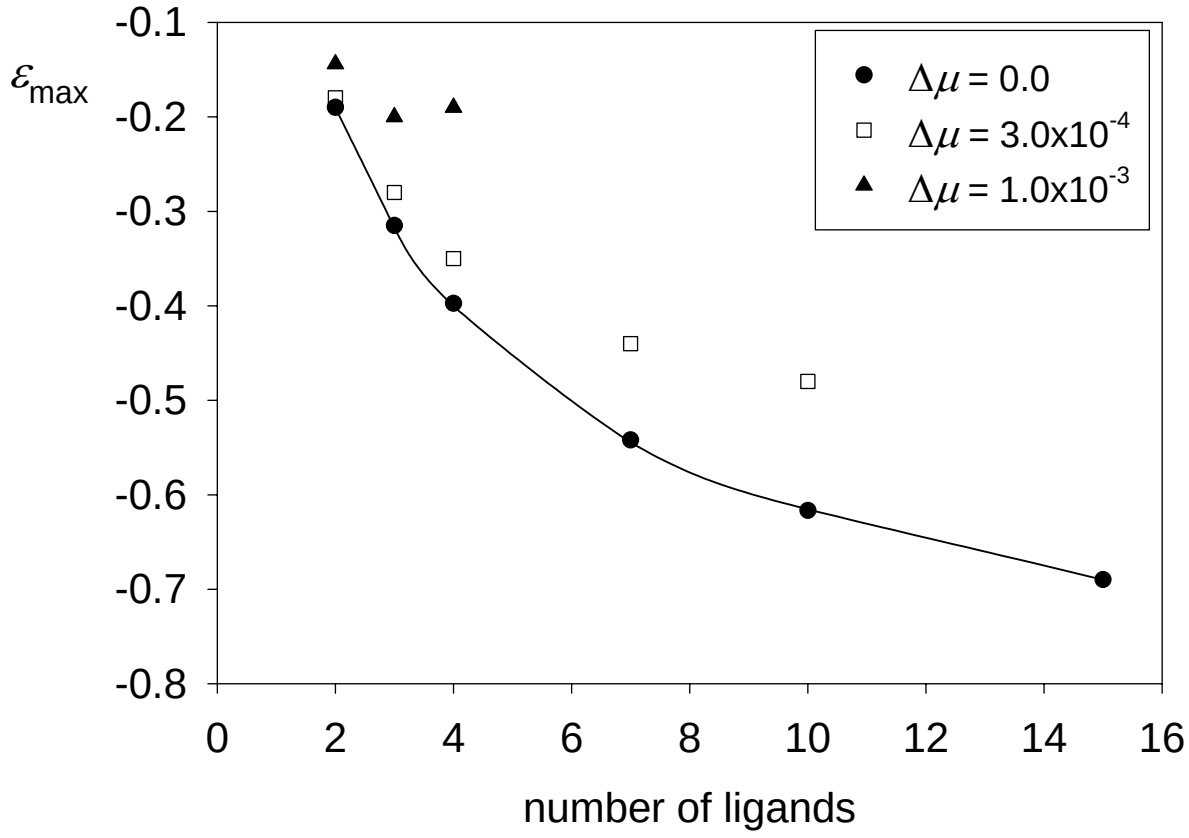

Fig. 9.

Published in Phys.Chem.Chem.Phys 2007, vol 9, p 2844-2855
DOI: 10.1039/b700913e

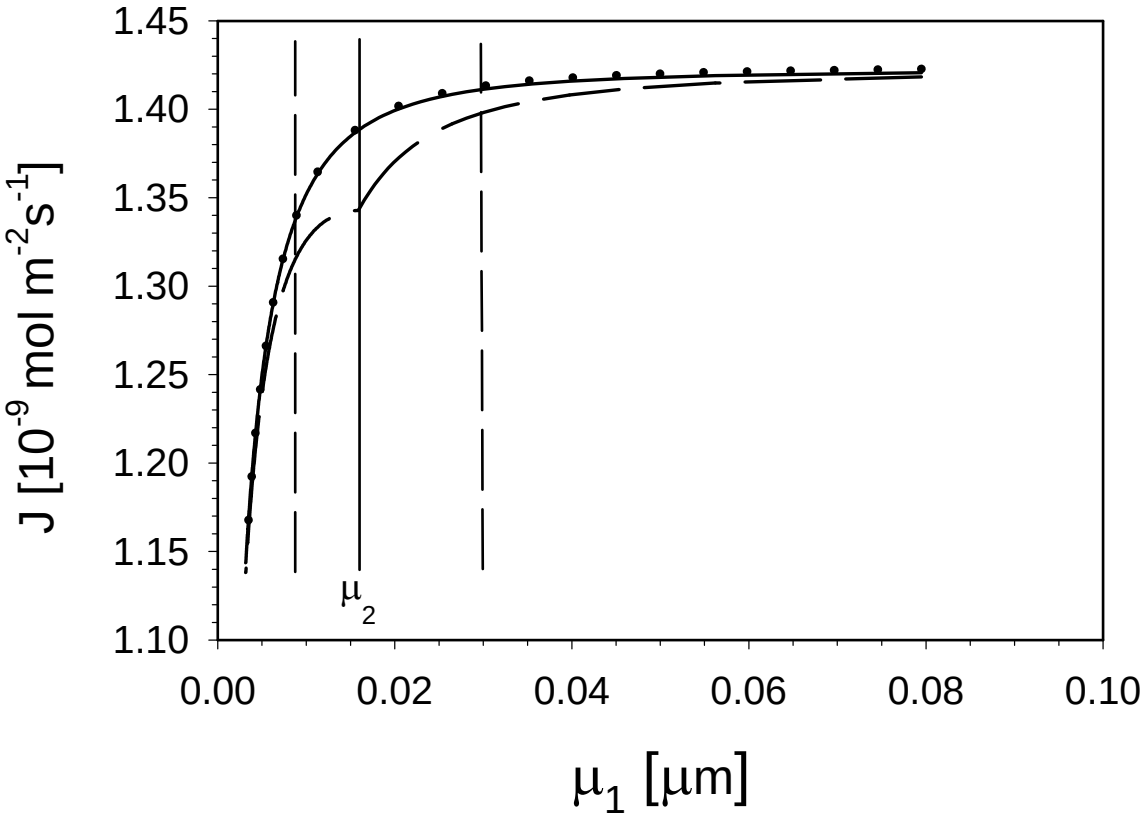

Figure 10

Published in Phys.Chem.Chem.Phys 2007, vol 9, p 2844-2855
DOI: 10.1039/b700913e

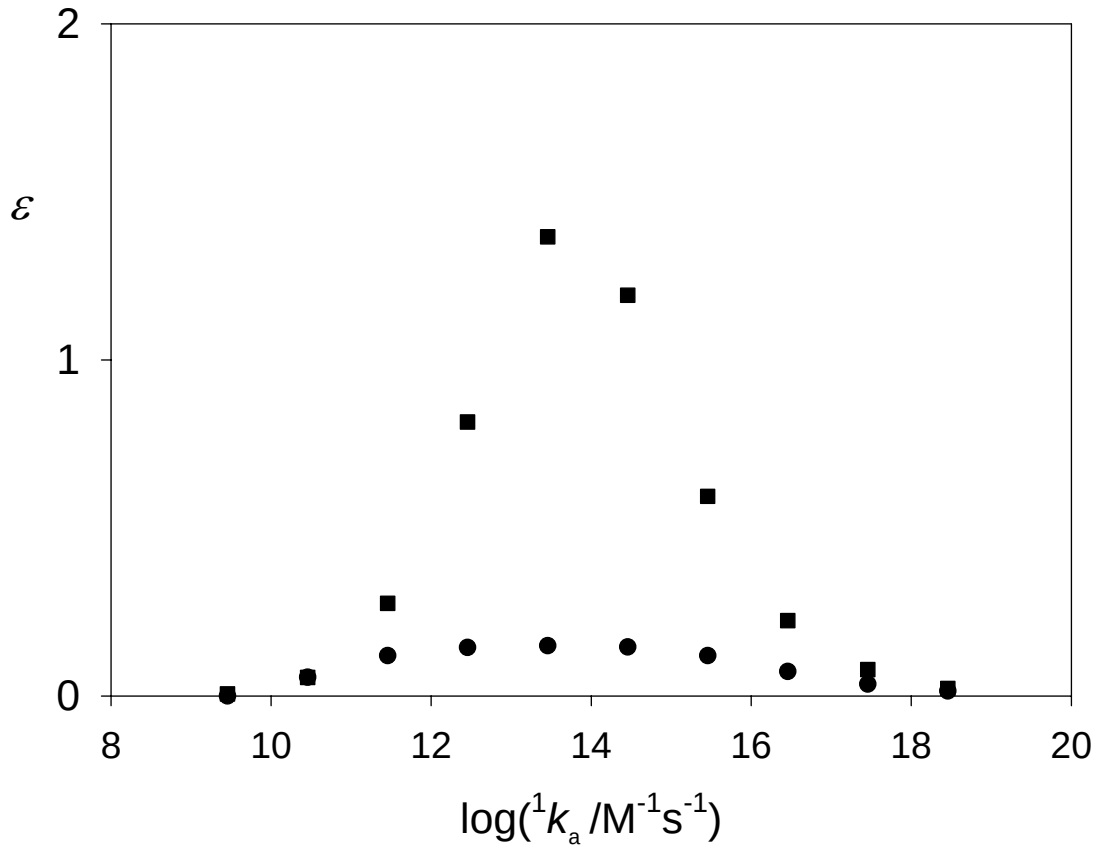

Fig. 11

Published in Phys.Chem.Chem.Phys 2007, vol 9, p 2844-2855
DOI: 10.1039/b700913e

References

1 K. J. Wilkinson, J. Buffle, in *Physicochemical kinetics and transport at chemical-biological surfaces.*,*Vol. 9* (Eds.: H. P. van Leeuwen, W. Koester), John Wiley, Chichester, UK, 2004, pp. 445-533.

2 M. Whitfield, D. R. Turner, in *Chemical Modeling in Aqueous Systems* (Ed.: E. A. Jenne), American Chemical Society, Washington DC, 1979, pp. 657-680.

3 J. Galceran, H. P. van Leeuwen, in *Physicochemical kinetics and transport at chemical-biological surfaces. IUPAC Series on Analytical and Physical Chemistry of Environmental Systems.*,*Vol. 9* (Eds.: H. P. van Leeuwen, W. Koester), John Wiley, Chichester, UK, 2004, pp. 147-203.

4 *In Situ Monitoring of Aquatic Systems. Chemical Analysis and Speciation. IUPAC Series on Analytical and Physical Chemistry of Environmental Systems.*, (Eds.: J. Buffle, G. Horvai) John Wiley & Sons, Chichester, 2000.

5 van Leeuwen, H. P., Town, R. M., and Buffle, J. Impact of ligand protonation on Eigen-type metal complexation kinetics in aqueous systems. (In press). Journal of Physical Chemistry . 2007.

6 D. R. Turner, in *Metal ions in biological systems. Vol 18* (Ed.: H. Sigel), Marcel Dekker, New York, 1984.

7 J. Buffle, M. L. Tercier-Waeber, *TrAC-Trends in Analytical Chemistry* 2005, **24**, 172-191.

8 H. P. van Leeuwen, R. M. Town, J. Buffle, R. Cleven, W. Davison, J. Puy, W. H. van Riemsdijk, L. Sigg, *Environ.Sci.Technol.* 2005, **39**, 8545-8585.

9 H. G. DeJong, H. P. van Leeuwen, *J.Electroanal.Chem.* 1987, **234**, 17-29.

10 K. Wiesner, *Chemicke Listy Pro Vedu A Prumysl* 1947, **41**, 6-8.

11 V. Hanus, *Chem.Zvesti* 1954, **8**, 702.

12 J. Koutecký, R. Brdicka, *Collect.Czech.Chem.Commun.* 1947, **12**, 337-355.

13 J. Koutecký, *Collect.Czech.Chem.Commun.* 1953, **18**, 597.

14 J. Koutecký, J. Koryta, *Electrochim.Acta* 1961, **3**, 318-339.

15 Z. Galus, *Fundamentals of Electrochemical Analysis*, Ellis Horwood, Chichester (UK), 1976.

16 Zhang, Z. S., Buffle, J., and van Leeuwen, H. P. Role of dynamic metal speciation and membrane permeability in the metal flux through lipophilic membranes. General theory and experimental validation with non labile complexes. Langmuir. In press. 2007.

17 J. Galceran, J. Puy, J. Salvador, J. Cecília, H. P. van Leeuwen, *J.Electroanal.Chem.* 2001, **505**, 85-94.

18 H. P. van Leeuwen, J. Puy, J. Galceran, J. Cecília, *J.Electroanal.Chem.* 2002, **526**, 10-18.

19 J. Salvador, J. Puy, J. Cecilia, J. Galceran, *J.Electroanal.Chem.* 2006, **588**, 303-313.

20 D. R. Turner, M. Whitfield, *J.Electroanal.Chem.* 1979, **103**, 43-60.

21 D. Alemani, B. Chopard, J. Galceran, J. Buffle, *Phys.Chem.Chem.Phys.* 2005, **7**, 3331-3341.

22 J. Galceran, J. Puy, J. Salvador, J. Cecília, F. Mas, J. L. Garcés, *Phys.Chem.Chem.Phys.* 2003, **5**, 5091-5100.

23 J. Salvador, J. L. Garces, J. Galceran, J. Puy, *J.Phys.Chem.B* 2006, **110**, 13661-13669.

24 Allison, J. D., Brown, D. S., and Novo-Gradac, K. J. MINTEQA2/PRODEFA2, A geochemical assessment model for environmental systems: version 3.0 user's manual. EPA 600/3-91/021; U.S. 1991. Washington, DC.7, U.S. Environmental Protection Agency, Office of Research and Development.

25 Puigdomenech, I. Medusa: make equilibrium diagrams using sophisticated algorithms. Windows program. 2001. Royal Institute of Technology KTH, Stockholm, Sweden.

26 Buffle, J. and Zhang, Z. S. Dynamic modelling of environmental metal complexes. In preparation. 2007.

27 D. Alemani, B. Chopard, J. Galceran, J. Buffle, *Phys.Chem.Chem.Phys.* 2006, **8**, 4119-4131.

28 J. Heyrovský, J. Kuta, *Principles of Polarography*, Academic Press, New York, 1966.

29 A. Tessier, J. Buffle, P. G. C. Campbell, in *Chemical and Biological Regulation of Aquatic Systems* (Eds.: J. Buffle, R. R. DeVitre), Lewis Publishers, Boca Raton, FL, 1994, pp. 197-230.

30 H. P. van Leeuwen, *Electroanal.* 2001, **13**, 826-830.

31 J. Puy, J. Cecília, J. Galceran, R. M. Town, H. P. van Leeuwen, *J.Electroanal.Chem.* 2004, **571**, 121-132.

32 J. Salvador, J. Puy, J. Galceran, J. Cecilia, R. M. Town, H. P. van Leeuwen, *J.Phys.Chem.B* 2006, **110**, 891-899.

33 Salvador, J., Garces, J. L., Galceran, J., Puy, J., and Town, R. M. Effect of the mixture on the lability of complexes (in preparation for J.Electroanal.Chem). 2007.